

# Cosmic Microwave Background

3/5

**Paolo de Bernardis**

Dipartimento di Fisica, Università La Sapienza, Roma

IV INPE Advanced School on Astrophysics

Radio Astronomy for the 21st Century

Sao Jose dos Campos

12/Sep/2011



SAPIENZA  
UNIVERSITÀ DI ROMA

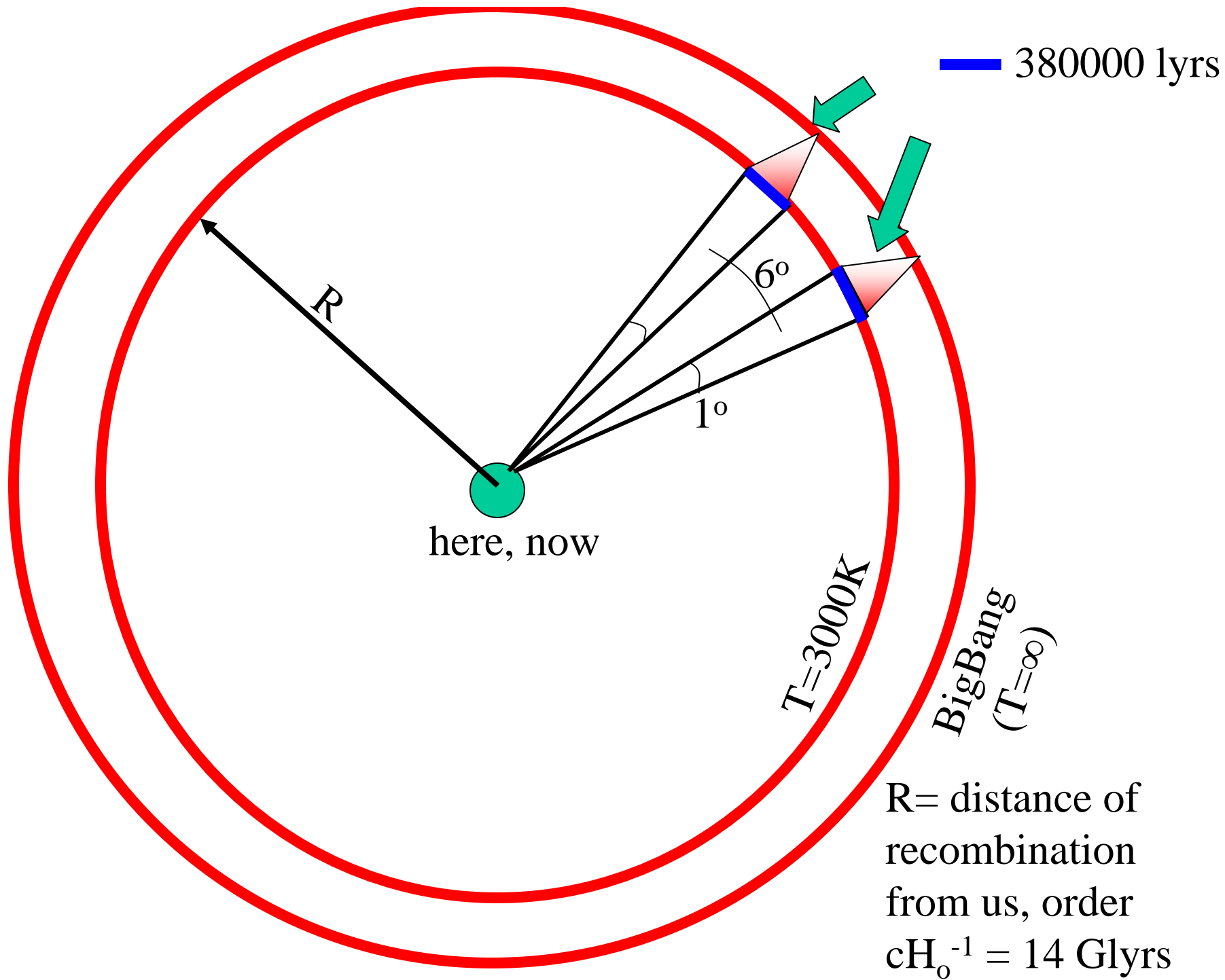


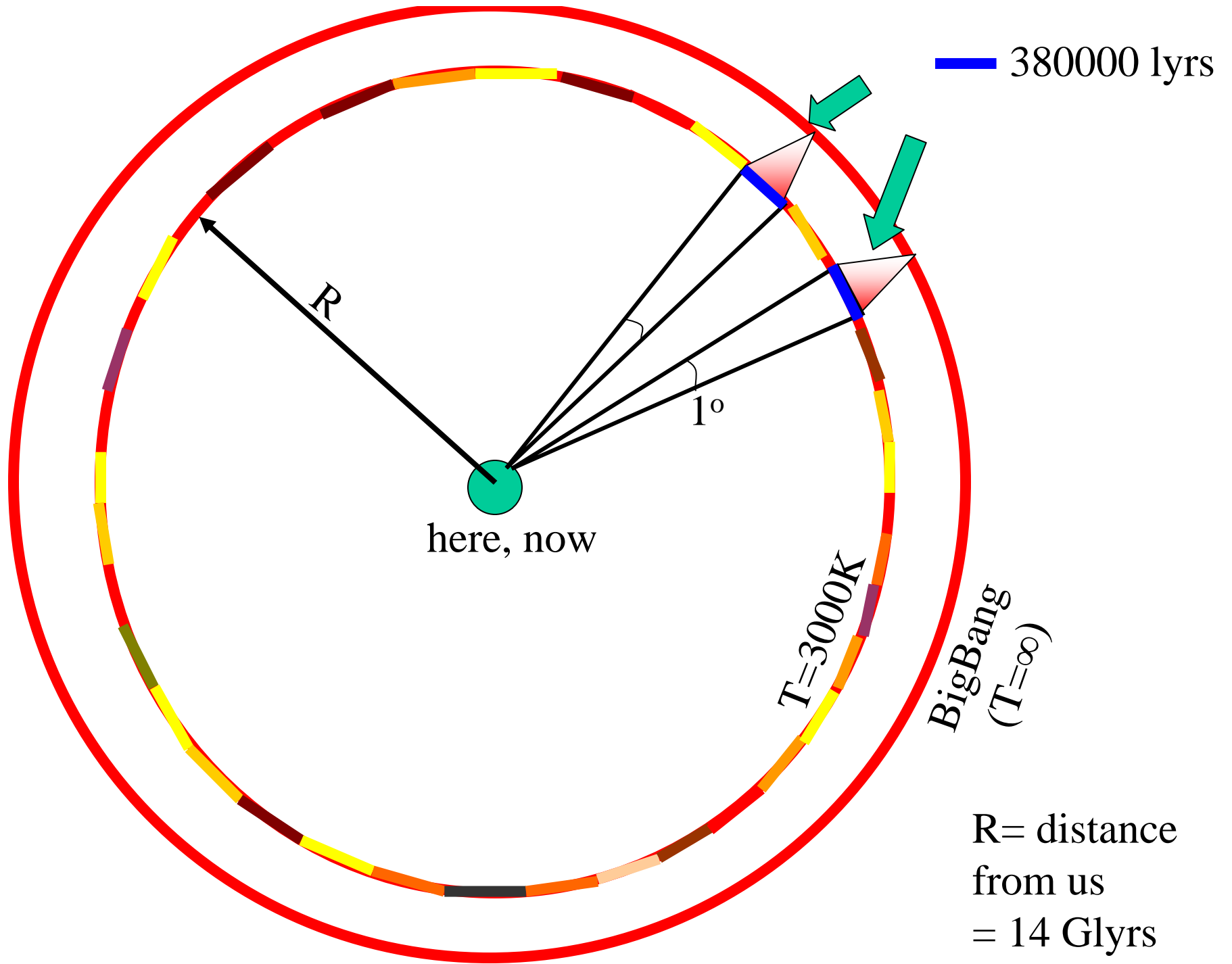
## Early measurements of CMB anisotropy

- Using the beam-switching technique described above, you can integrate for some time on one couple of directions, then change directions and integrate again, then change ... until you get a statistical sample of the sky, consisting typically in a few tens to a few hundreds directions.
- This is enough to estimate the rms fluctuation of the temperature (brightness) of the sky, extracting it from the noise.
- These experiments started immediately after the discovery of the CMB (Penzias and Wilson stated in the discovery paper of 1965 that it was isotropic to 10%)... and were very frustrating !
- For more than two decades a few groups of pioneers of the CMB improved their isotropometers, obtaining increasingly stringent upper limits for the anisotropy of the CMB, down to a level

$$\frac{\Delta T}{T} < 10^{-4}$$

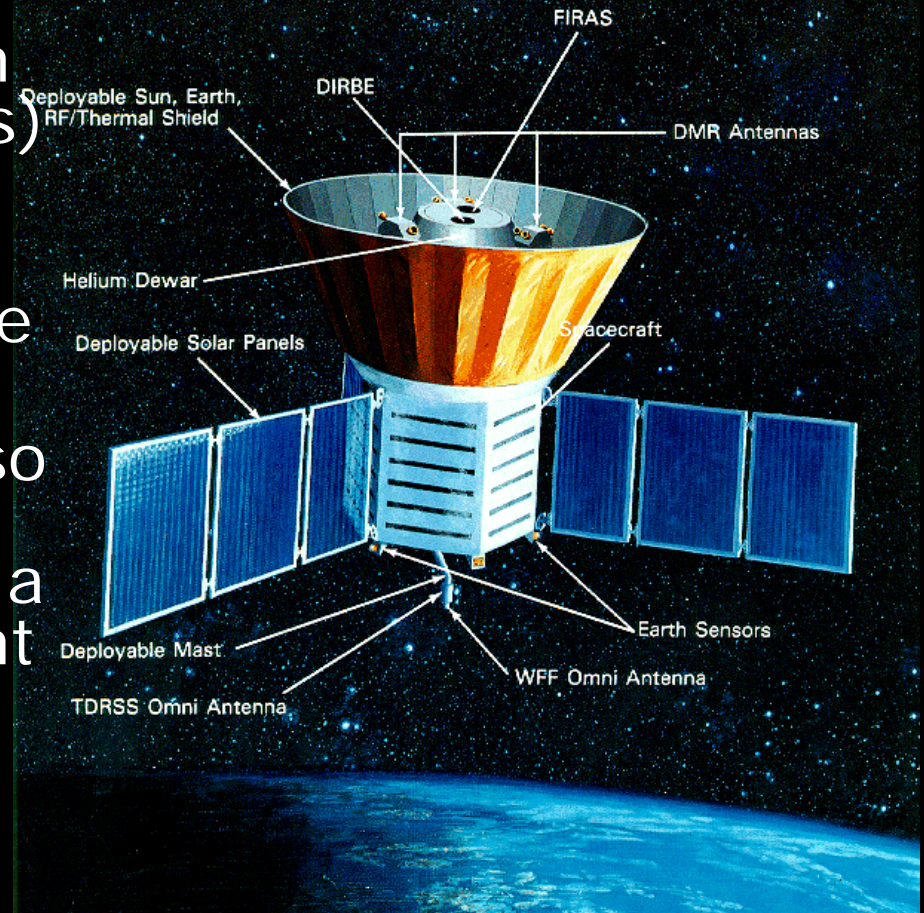
at scales of the order of the horizon. So regions which have never been in causal contact before produce the same CMB brightness, with outstanding precision. How is this possible ? This is the paradox of horizons.

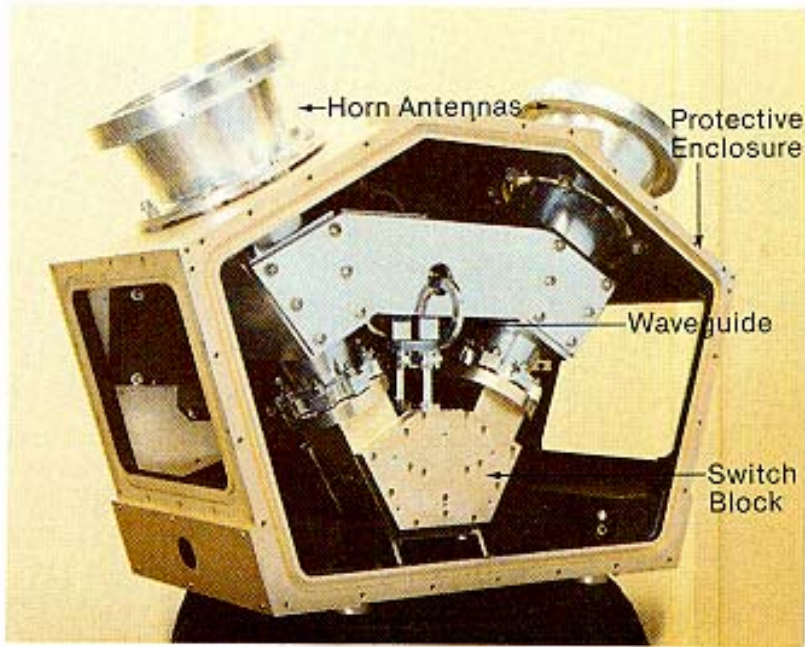




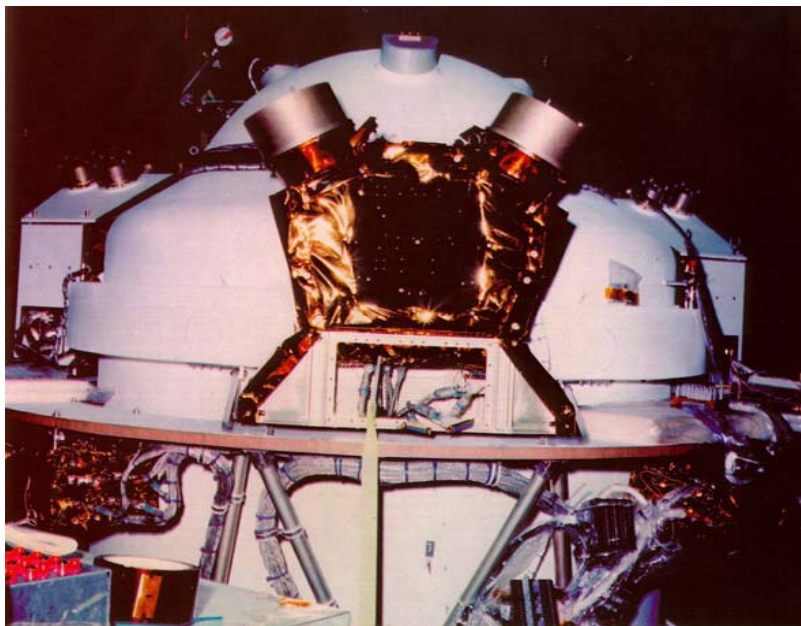
# 1992 : COBE-DMR

- COBE-DMR was a set of 3 differential radiometers aboard of the COBE satellite.
- Each radiometer had two horn antennas and a switch to measure the difference in sky temperature (brightness) between two directions  $60^\circ$  apart.
- The angular resolution of the antennas was  $7^\circ$  FWHM.
- The satellite was spinning, so each differential radiometer scanned the sky, producing a large number of independent difference measurements, which were eventually converted into maps of the microwave sky at 31.5, 53, 90 GHz, with a resolution around  $10^\circ$

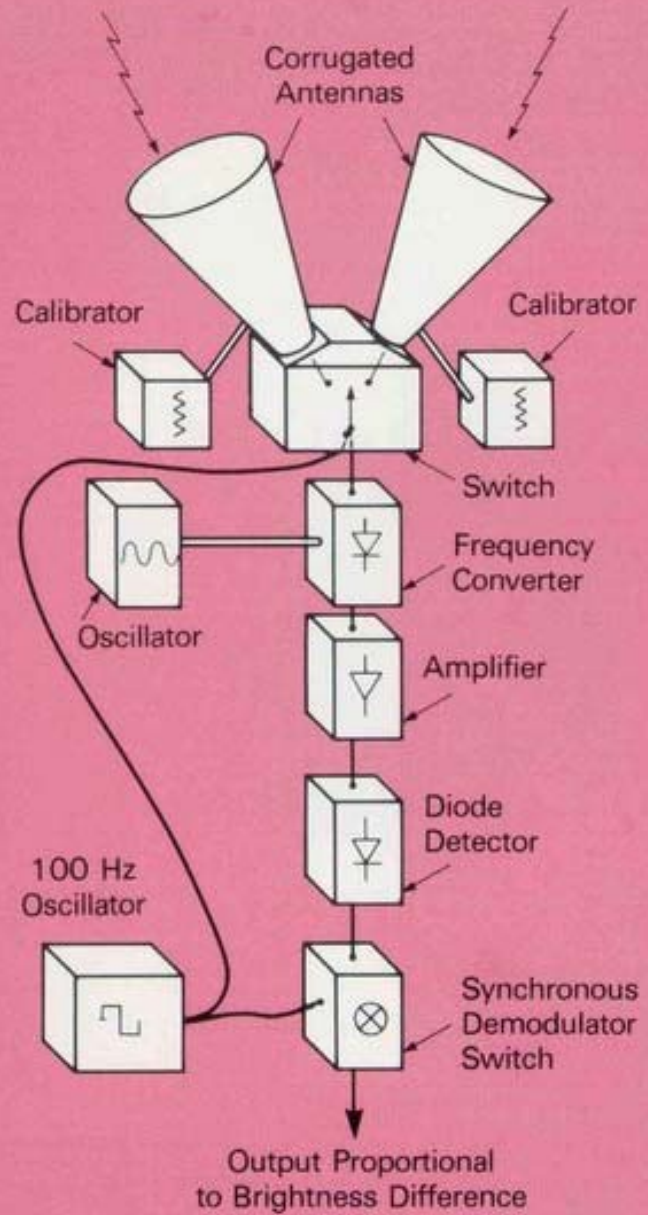




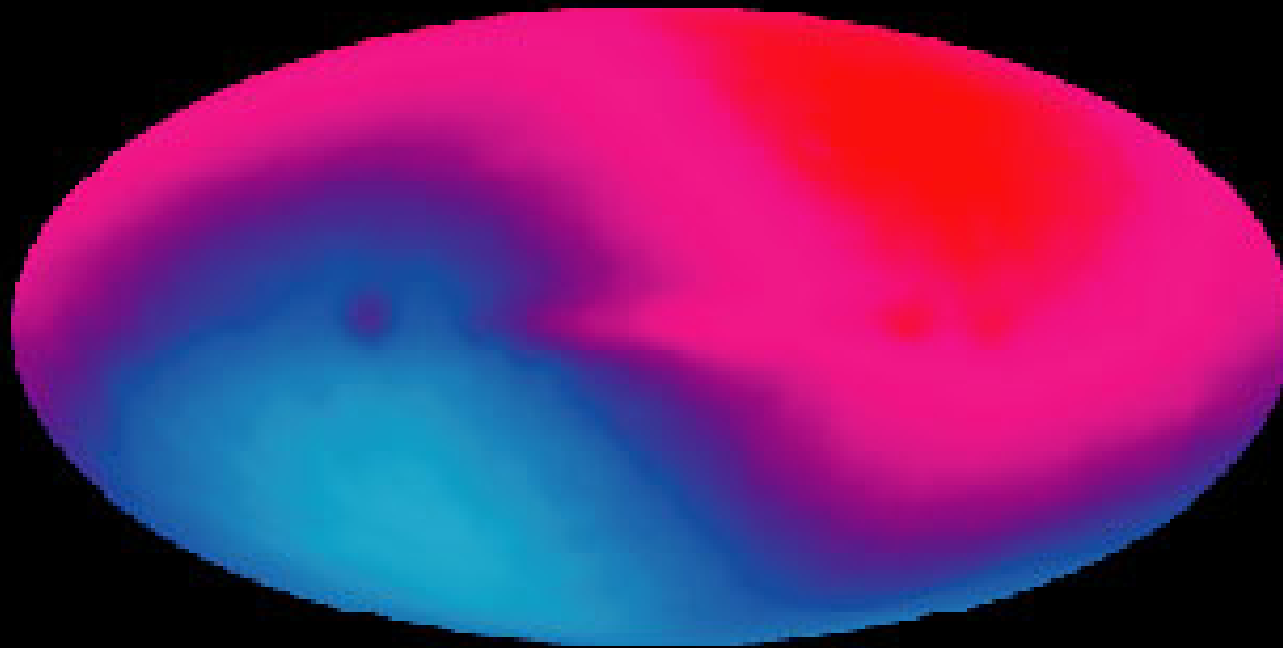
The 9.6 mm DMR receiver partially assembled. Corrugated cones are antennas.



### DMR Signal Flow Diagram



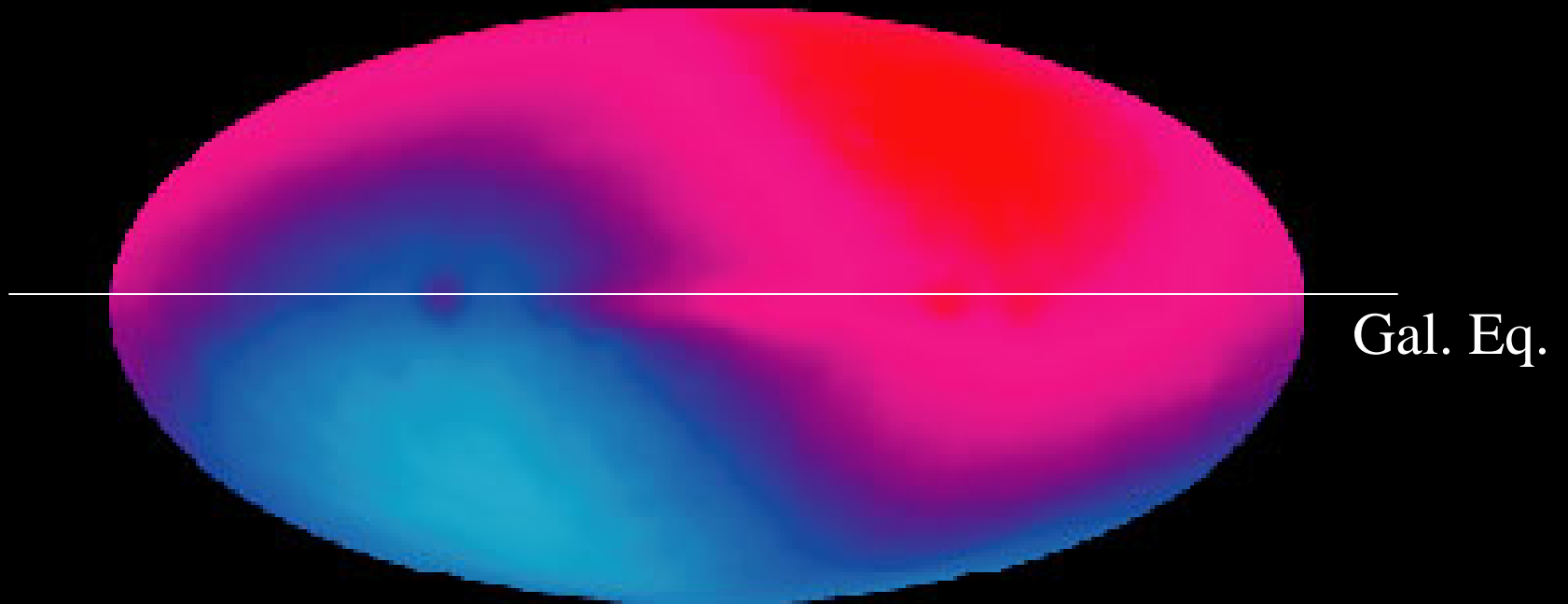
- COBE map of the whole sky :  
Red :  $\Delta T = + 3 \text{ mK}$   
Blue :  $\Delta T = - 3 \text{ mK}$



- COBE map of the whole sky

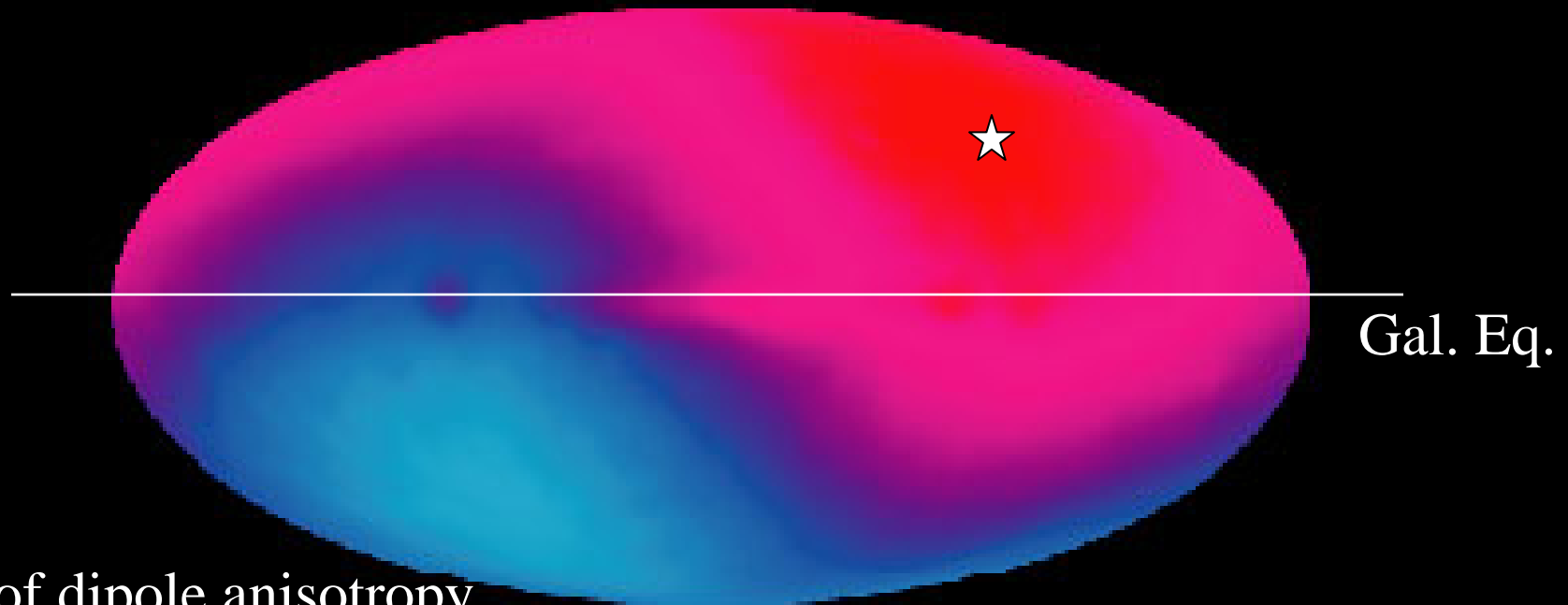
Red :  $\Delta T = + 3 \text{ mK}$

Blue :  $\Delta T = - 3 \text{ mK}$



- COBE map of the whole sky

Red :  $\Delta T = + 3 \text{ mK}$   
Blue :  $\Delta T = - 3 \text{ mK}$



★ apex of dipole anisotropy  
(WMAP)  
 $l=(263.85_{\pm 0.1})^\circ$   
 $b=(48.25_{\pm 0.04})^\circ$   
(close to the ecliptic...)

Amplitude of dipole anisotropy  
(WMAP)  
 $\Delta T=(3.346_{\pm 0.017})\text{mK}$

# Derivation of the CMB dipole

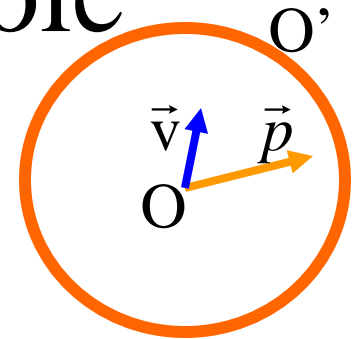
- We are moving with a velocity  $v$  with respect to the CMB Last Scattering Surface.
- The CMB is isotropic in the reference frame  $O'$  of the LSS, but is not isotropic in the restframe  $O$  of the observer, which is in motion.
- The distribution function  $f$  of particles with momentum  $\mathbf{p}$  is a Lorentz invariant: In fact

$$f(\mathbf{p}) = \frac{dN}{dx^i dp^i}$$

where  $dN$  is a scalar, so is invariant, and the phase space volume  $dx^i dp^i$  can also be shown to be a Lorentz invariant. So

$$f'(\mathbf{p}') = f(\mathbf{p})$$

# Derivation of the CMB dipole



- The Lorentz transformation for the momentum  $\mathbf{p}$  is

$$c\vec{p} = \frac{\sqrt{1 - v^2 / c^2}}{1 - \vec{v} \times \vec{n} / c} c\vec{p}' \quad \vec{n} = \vec{p} / p$$

- Applying this eq. to the Planck distribution function for photons we get

$$T = \frac{p}{p'} T' \Rightarrow T = \frac{\sqrt{1 - v^2 / c^2}}{1 - \vec{v} \times \vec{n} / c} T' = \frac{\sqrt{1 - \beta^2}}{1 - \beta \cos(\theta)} T'$$

- This formula was first derived by Mosengheil (1907), and rederived by Peebles and Wilkinson (1968), Heer and Kohl (1968), Forman (1970).

- For small  $\beta$ :

$$T(\theta) \cong T_o \left[ 1 + \beta \cos(\theta) + \frac{\beta^2}{2} \cos(2\theta) \right]$$

kinematic  
term

light aberration  
term

$\beta$

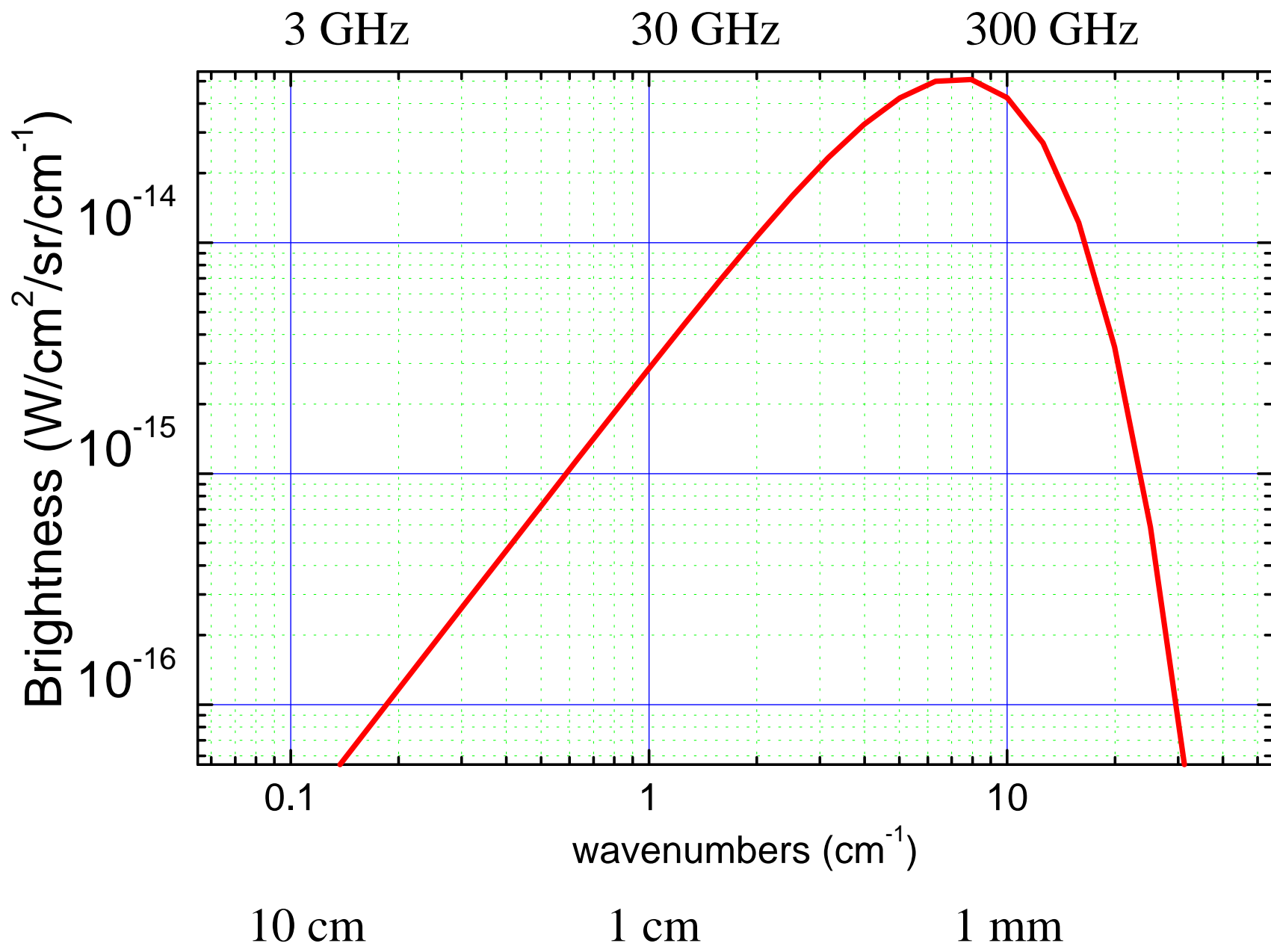
- The motion of the Earth with respect to the CMB is the combination of
  - The motion of the Earth around the Sun (well known)
  - The motion of the Sun in the Galaxy (well known)
  - The motion of the Galaxy in the Local Group (known)
  - The bulk motion of the Local Group (not well known) due to the gravitational acceleration generated by all other large masses present in the Universe
- The annual revolution of the Earth around the Sun is known extremely well ( $v \sim 30$  km/s), and produces an **annual modulation in the CMB dipole**. This is the main signal used in COBE and WMAP for the Dipole calibration, since it is known from astrometric measurements, much better than the total motion of the earth.
- This effect produces a modulation of the order of  $\beta T_o$ , i.e. about  $300\mu\text{K}$ , on a total dipole of the order of  $3.5$  mK.

# CMB dipole signal

- The CMB temperature fluctuation corresponds to a CMB brightness fluctuation, which can be found by deriving the Planck formula with respect to T:

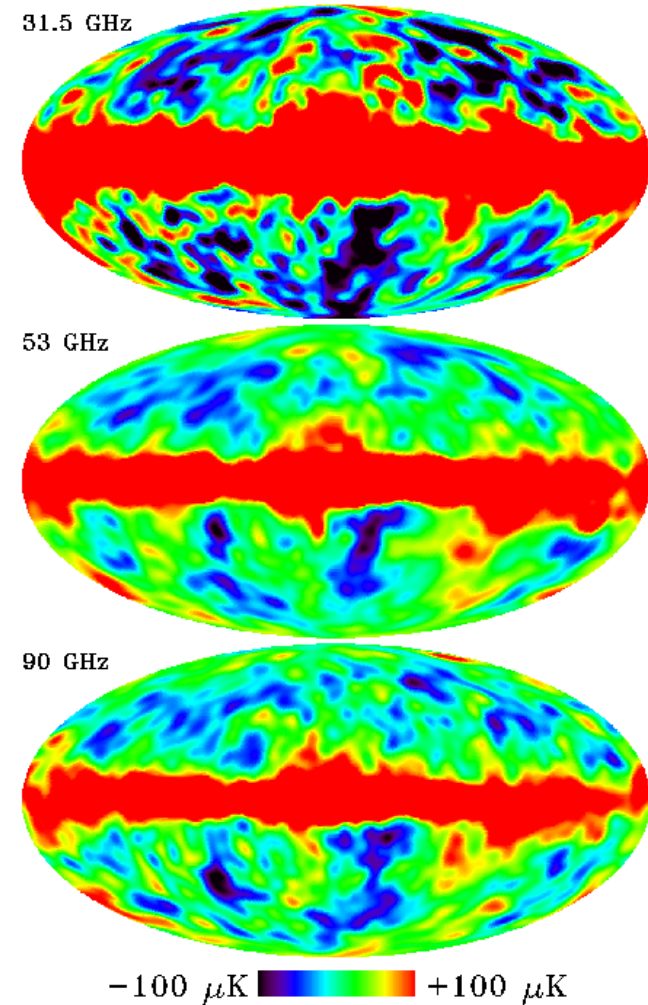
$$\Delta I = \frac{x e^x}{e^x - 1} B(T_{CMB}, \nu) \Delta T \quad ; \quad x = \frac{h \nu}{k T_{CMB}}$$

- This conversion from Temperature to Brightness is the same for the dipole and for any smaller scale temperature or polarization anisotropy. For this reason the Dipole spectrum is the same as the spectrum of CMB anisotropy. The maximum of this spectrum is at 271 GHz.



# Large-Scale Anisotropy

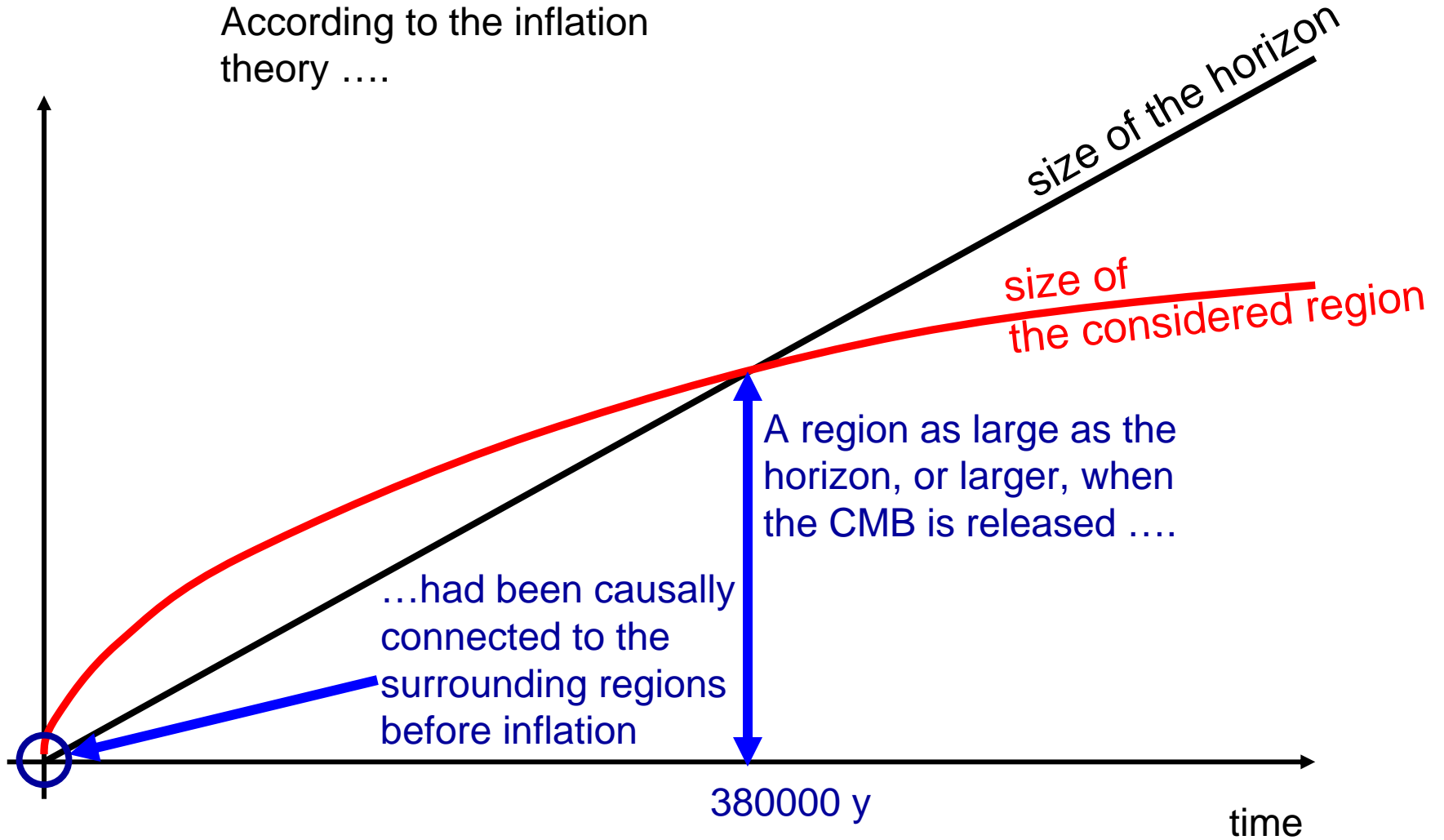
- Removing the dipole component, COBE-DMR detects a small (10ppm rms) large-scale anisotropy of the CMB.
- This incredible smoothness *requires* an **inflationary process**, happening in the first split second after the Big Bang, and causally connecting regions which, at recombination, are separated more than the horizon.

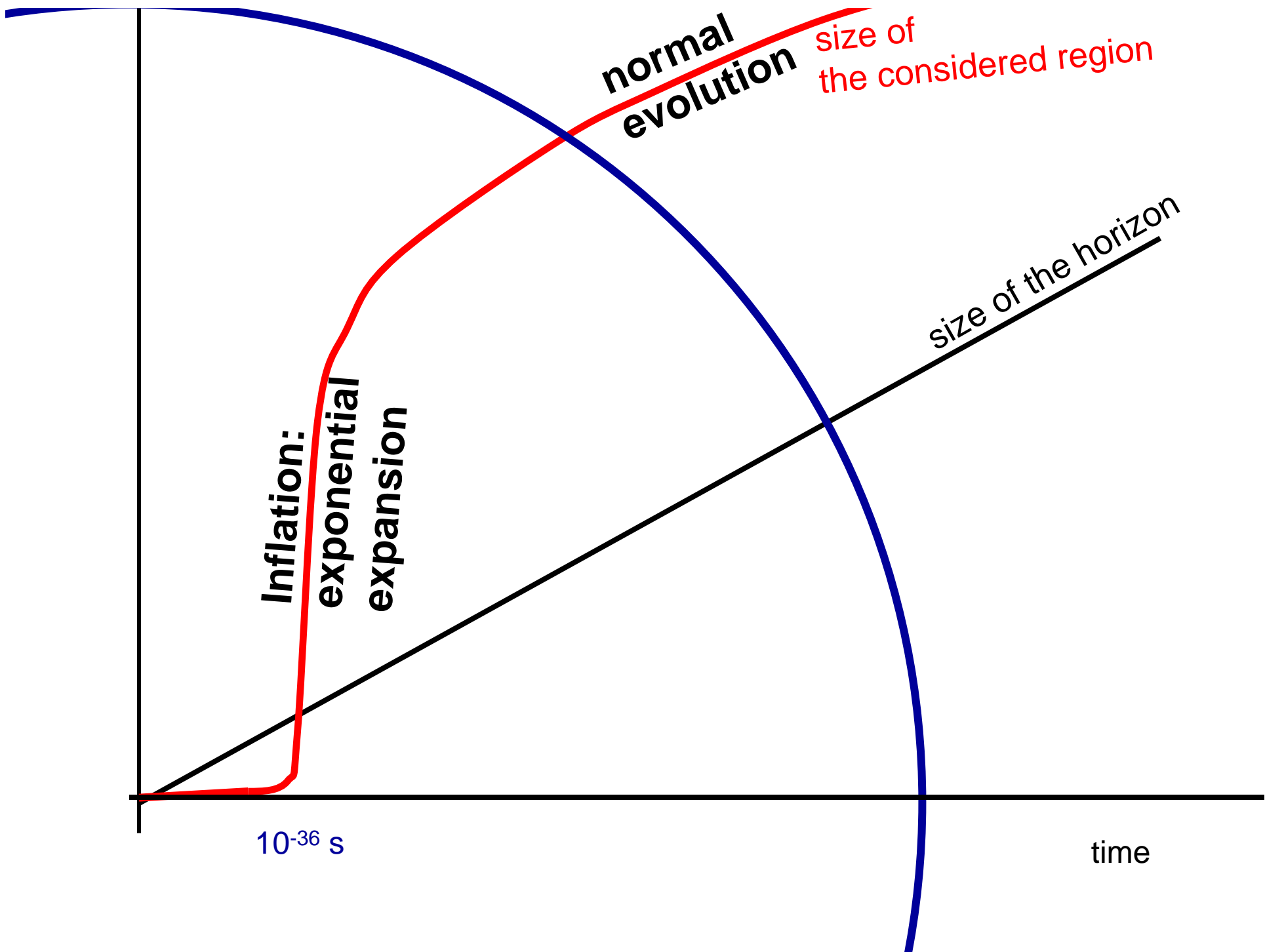


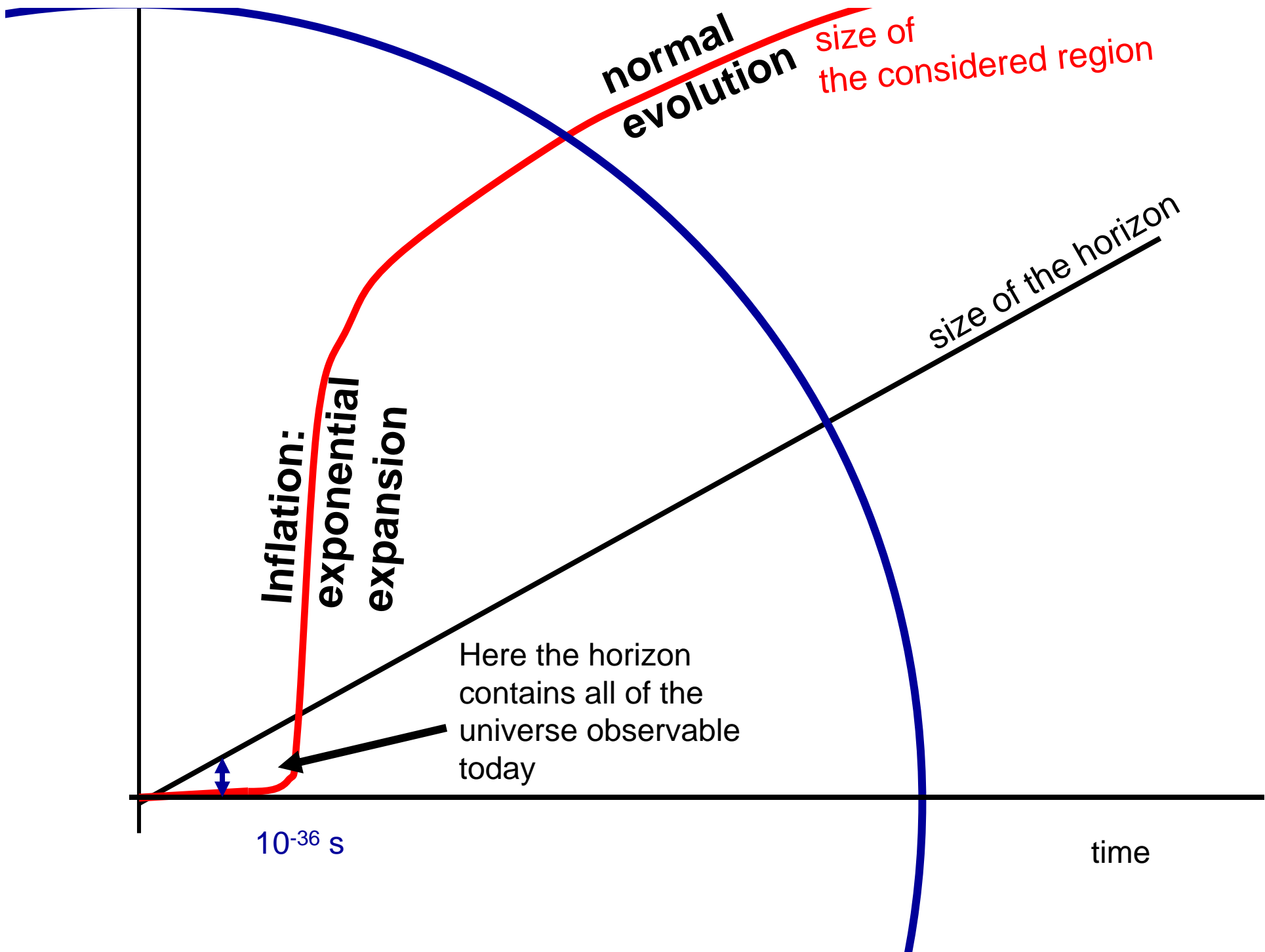
G. Smoot et al. 1992, Nobel Prize in 2006

# Expansion vs Horizon

According to the inflation theory ....





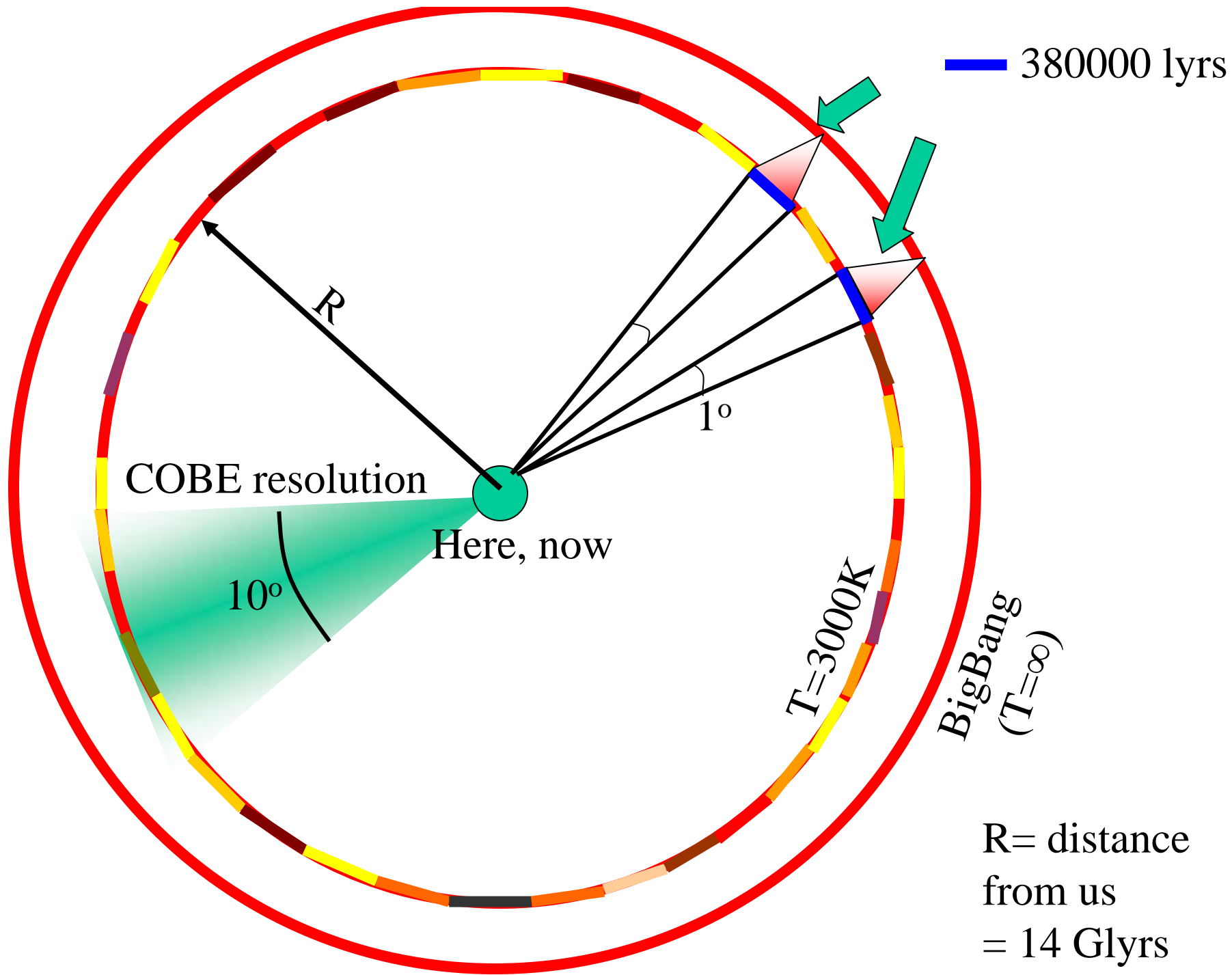


# Inflation

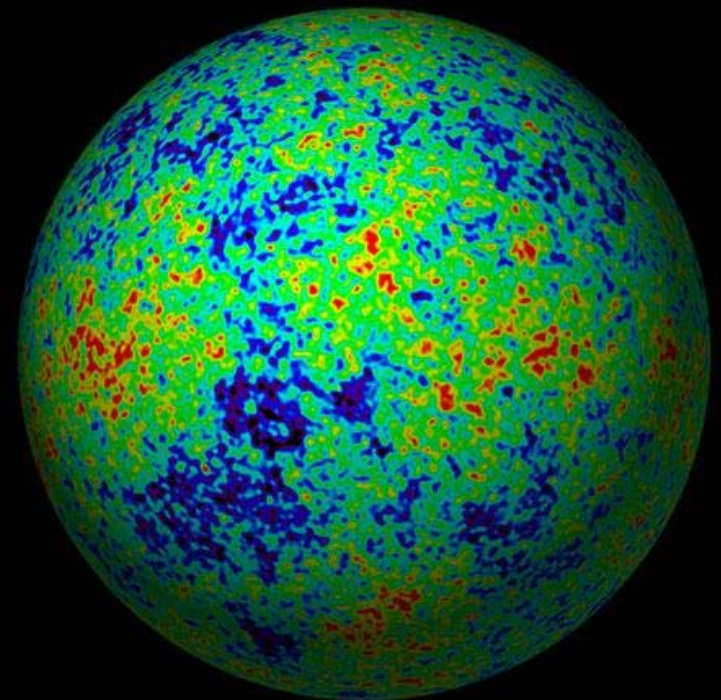
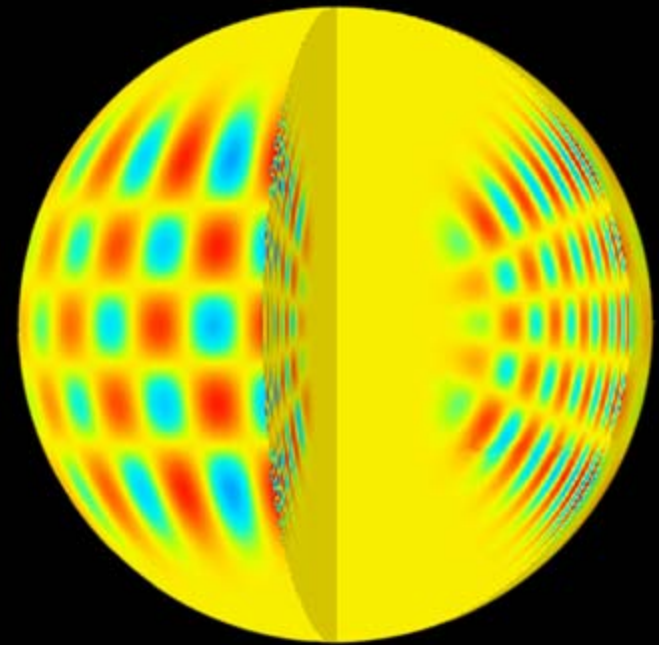
- Inflation is produced by a phase transition in the very early universe, resulting in a very short period of exponential expansion of space.
- It was introduced to solve the paradox of horizons, but also to solve other problems: the paradox of flatness, the paradox of magnetic monopoles, ...
- .. and to provide a physical origin for the density fluctuations producing large-scale structures in the universe.
- As we will see later, inflation is a *predictive* theory, and most of its predictions have been *tested* quite deeply.
- But let's go back to CMB measurements.

# The quest for sensitivity and angular resolution.

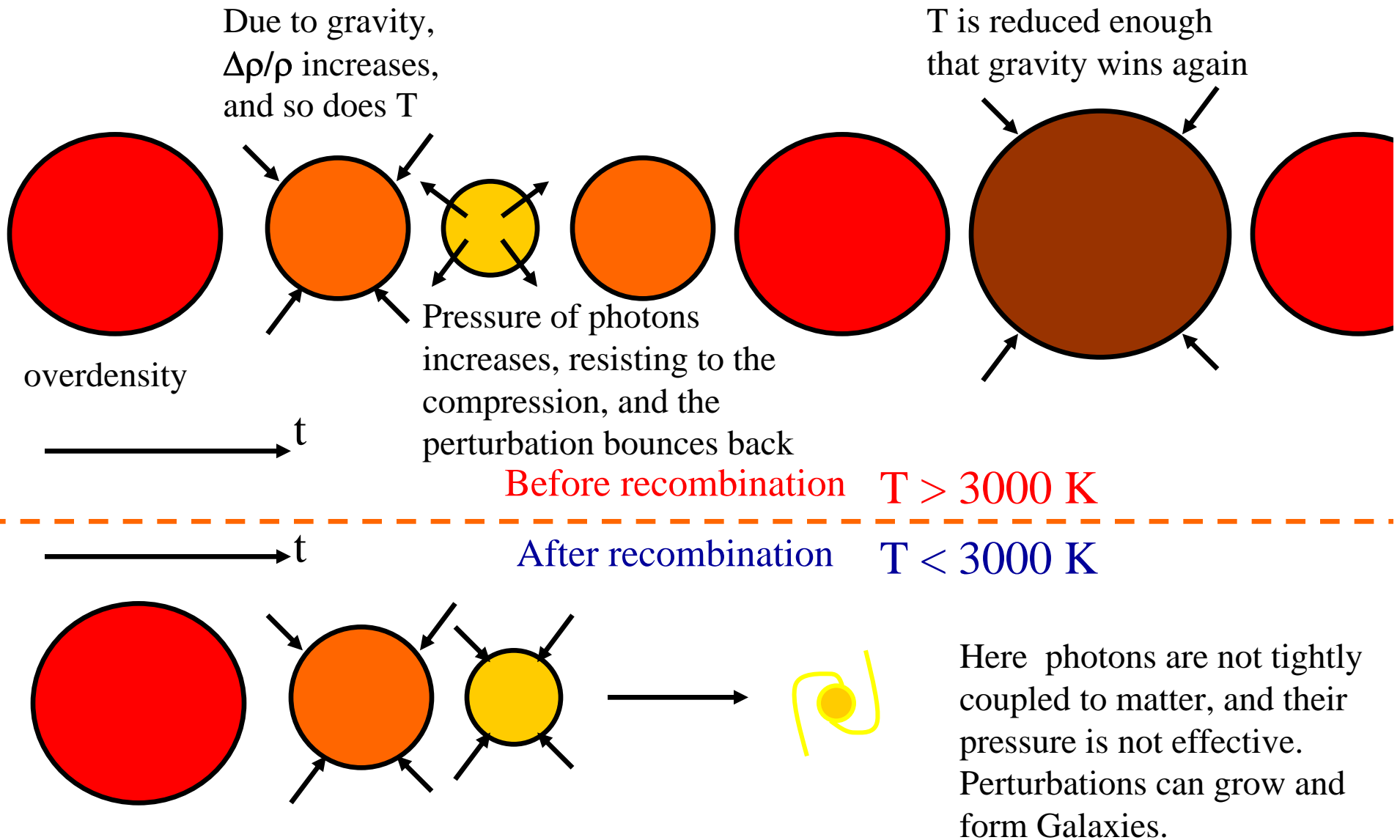
- Having solved the paradox of horizons, we still have a long time (basically all the 380000 years of the primeval fireball before recombination) in which horizon-sized regions evolve independently.
- We still expect to see the characteristic size of the horizon at recombination imprinted in the microwave sky, even if not dramatically as in the paradox of horizons.
- COBE-DMR was on-board of a small satellite, and did not have large telescopes, only feed-horns directly looking at the sky, limiting its resolution to  $7^\circ$  FWHM .
- This was not sufficient to measure degree-sized horizons..



- The study of solar oscillations allows us to investigate the interior structure of the sun, well below the solar photosphere.
- The study of CMB anisotropy allows us to investigate the oscillations of the primeval plasma, and the universe well behind (well before) the cosmic photosphere (the recombination epoch)



Density perturbations ( $\Delta\rho/\rho$ ) were **oscillating** in the primeval plasma (as a result of the opposite effects of gravity and photon pressure).



After recombination, **density perturbation** can **grow** and create the hierarchy of structures we see in the nearby Universe.

- The brightness (temperature) fluctuations are due to small density fluctuations present in the primeval fireball, and to their motions:

$$\frac{\Delta T}{T} = \frac{1}{4} \frac{\Delta \rho_\gamma}{\rho_\gamma} + \frac{1}{3} \frac{\Delta \phi}{c^2} + \frac{v}{c}$$

Photon  
Density  
fluctuations

Gravitational  
redshift

Scattering  
against  
moving  $e^-$

- Overdensity : Gravitational redshift :

$$\frac{\delta T}{T} = -\frac{\delta\Phi}{c^2}$$

- Overdensity : time delay

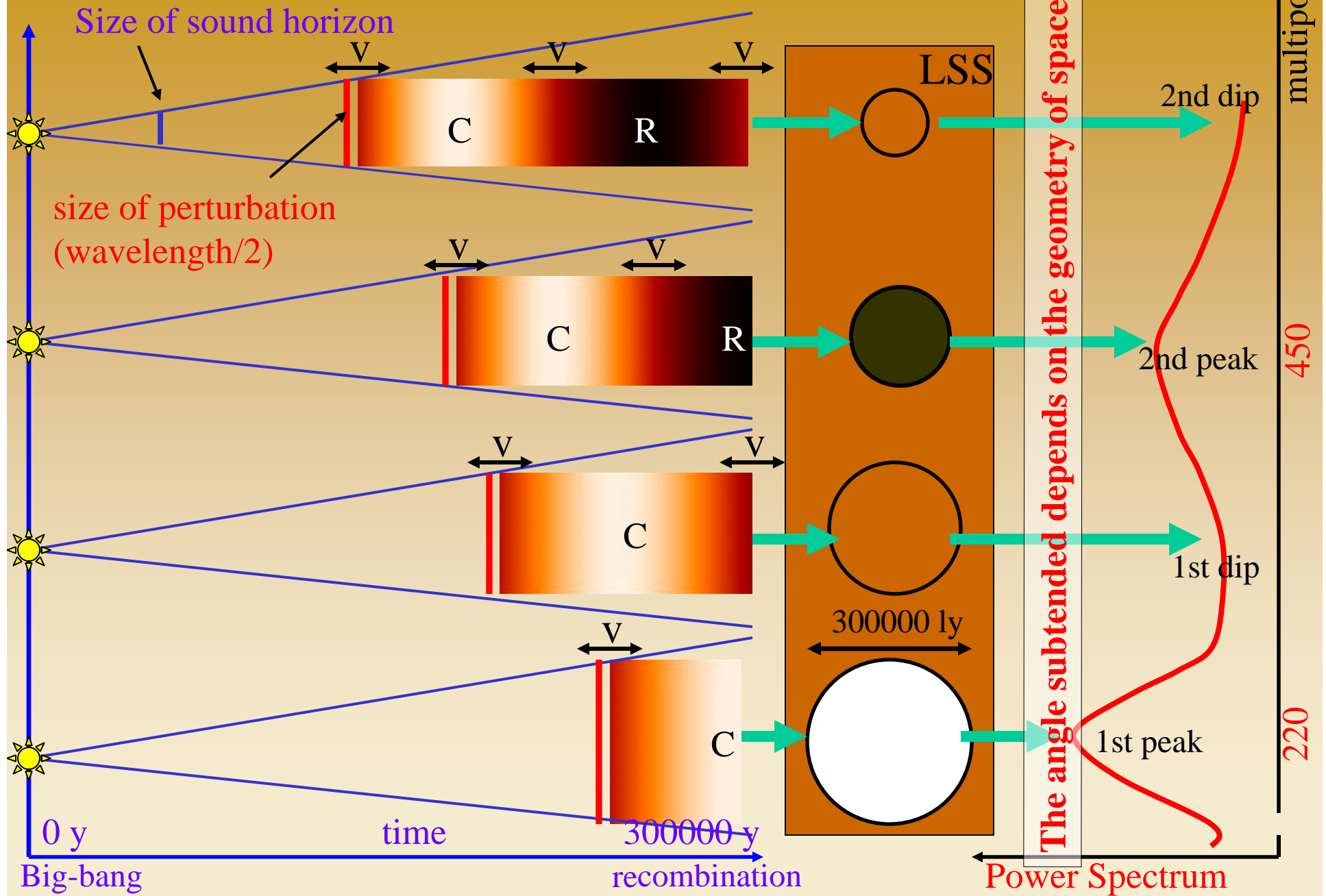
$$\frac{\delta t}{t} = -\frac{\delta\Phi}{c^2}$$

- During the matter-dominated phase:

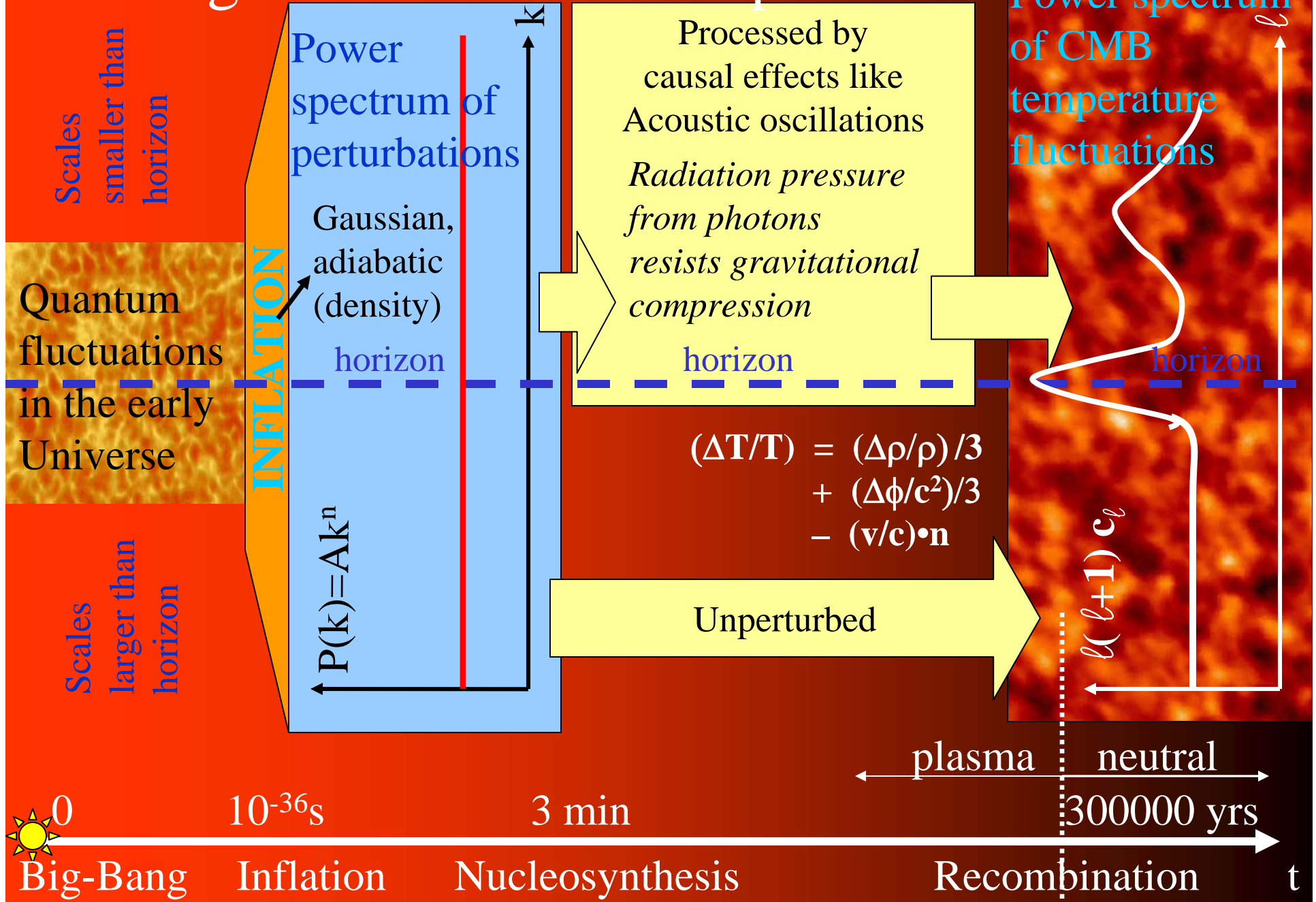
$$T \propto 1/a \quad ; \quad a \propto t^{2/3} \quad \rightarrow \quad \frac{\delta T}{T} = -\frac{\delta a}{a} = -\frac{2}{3} \frac{\delta t}{t} = \frac{2}{3} \frac{\delta\Phi}{c^2}$$

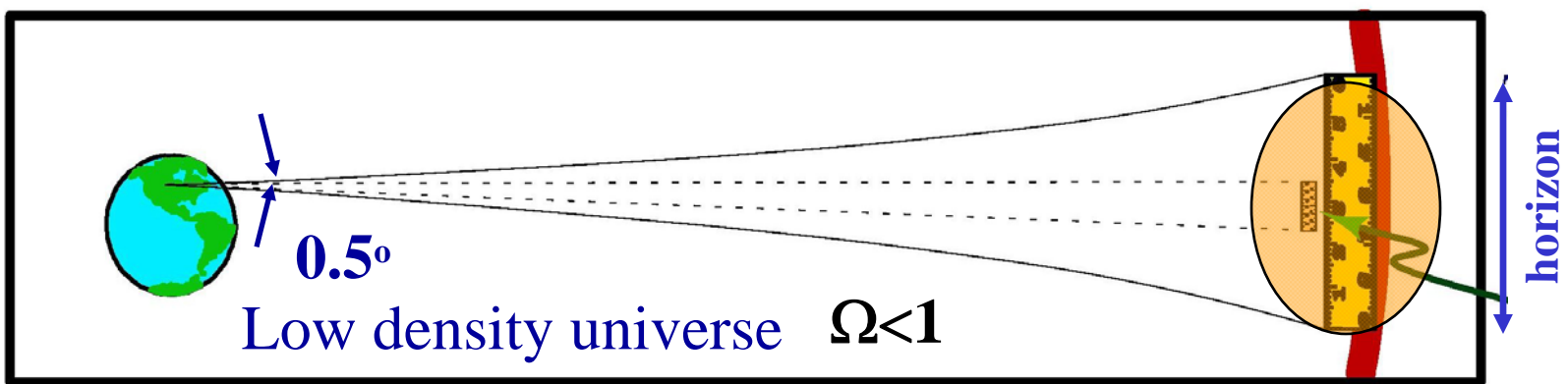
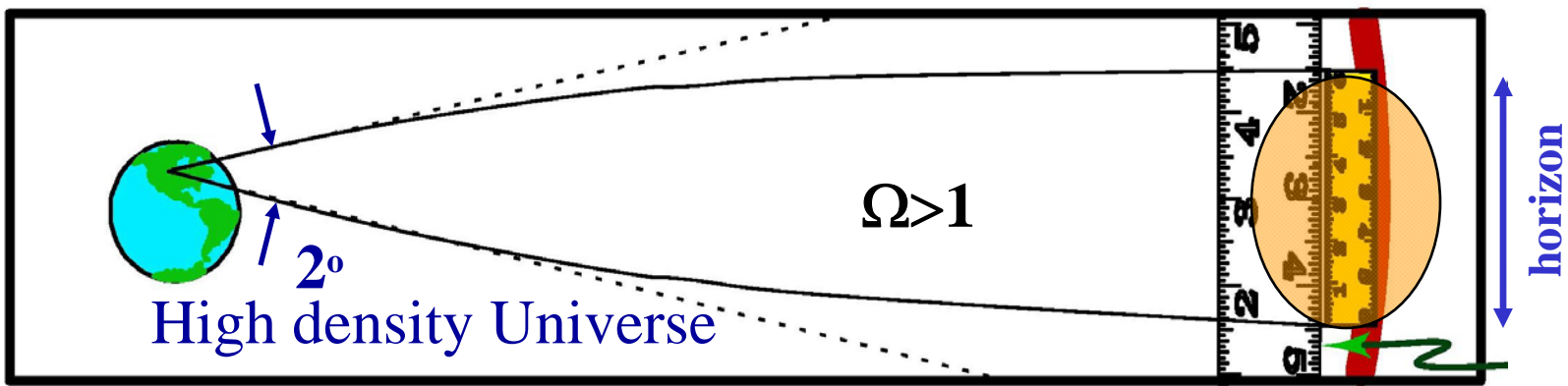
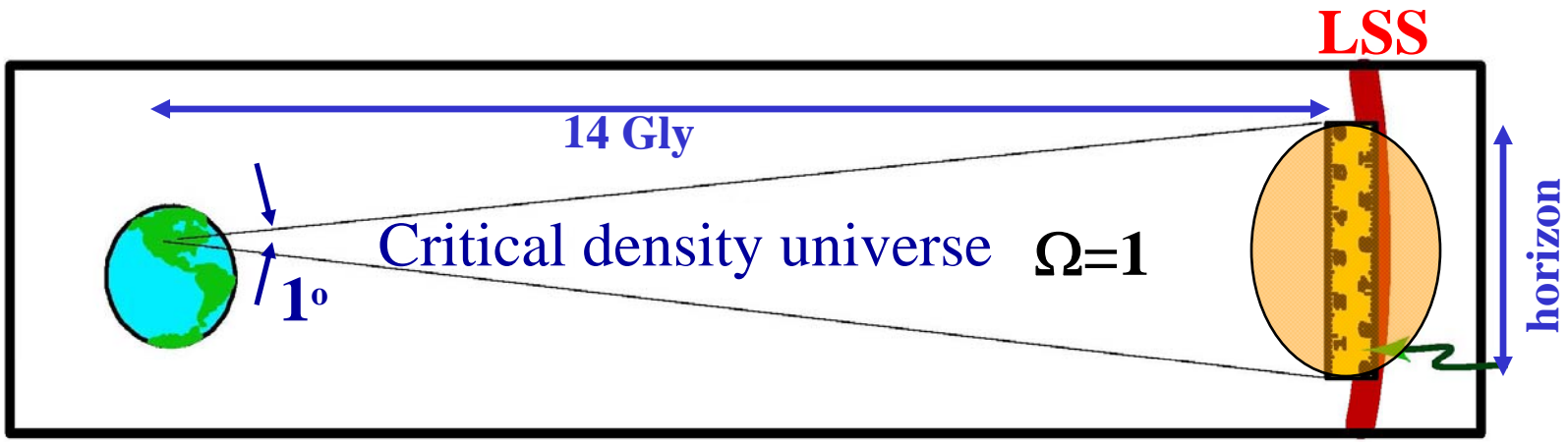
- So, in total  $\frac{\delta T}{T} = -\frac{1}{3} \frac{\delta\Phi}{c^2}$       Sachs-Wolfe Effect (1967)

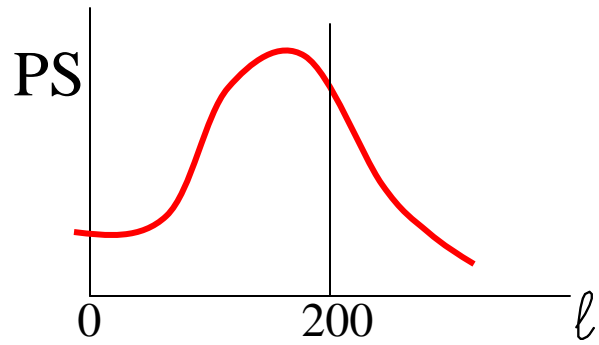
In the primeval plasma, photons/baryons density perturbations start to oscillate only when the sound horizon becomes larger than their linear size. Small wavelength perturbations oscillate faster than large ones.



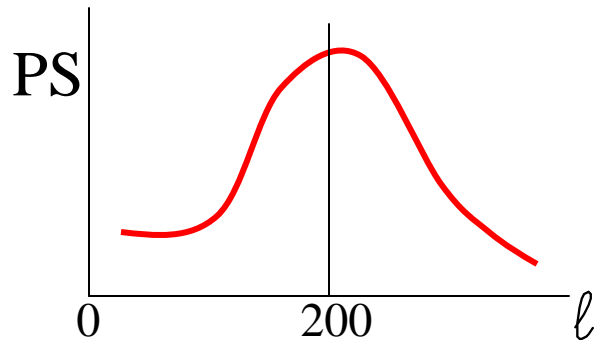
# Paradigm of CMB anisotropies



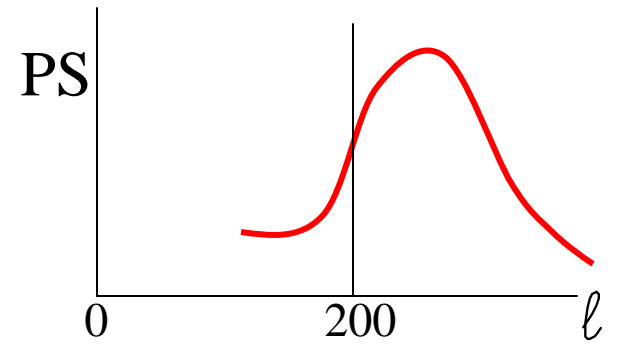




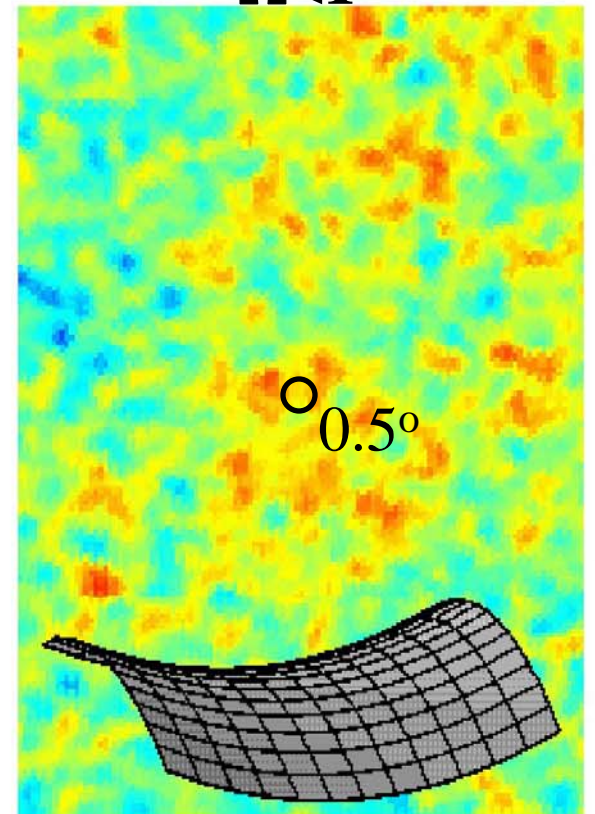
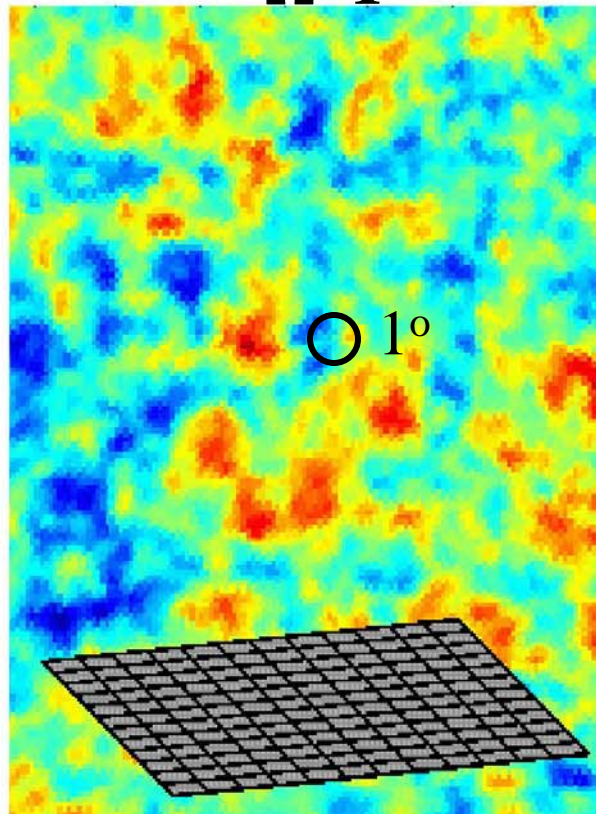
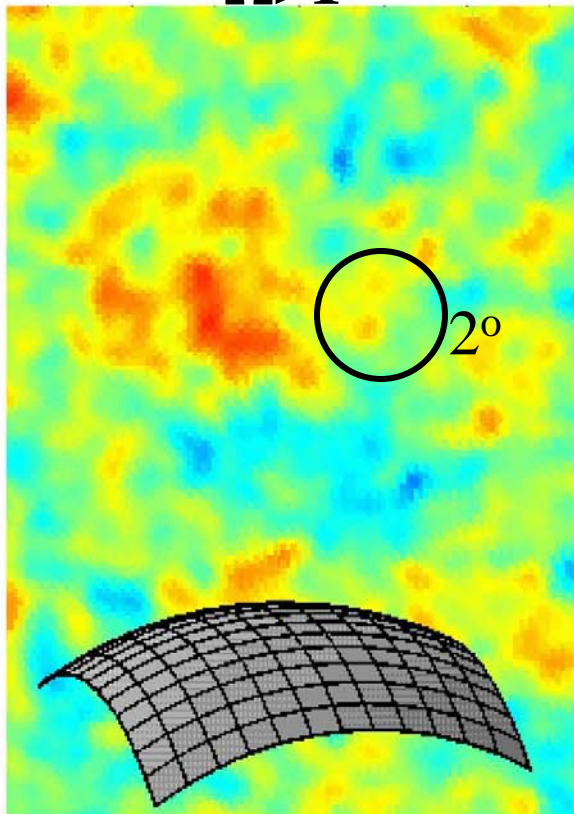
High density Universe  
 $\Omega > 1$



Critical density Universe  
 $\Omega = 1$



Low density Universe  
 $\Omega < 1$



# The quest for high angular resolution

- The **angular power spectrum**  $c_\ell$  of the anisotropy defines the contribution to the rms  $\Delta T$  from the different multipoles:

$$\Delta T(\theta, \varphi) = \sum_{\ell, m} a_{\ell m} Y_\ell^m(\theta, \varphi)$$

$$c_\ell = \langle a_{\ell m}^2 \rangle$$

$$\langle \Delta T^2 \rangle = \frac{1}{4\pi} \sum_\ell (2\ell + 1) c_\ell$$

- A real experiment will not be sensitive in the same way to all the multipoles of the CMB, because it has a finite angular resolution, i.e. the response to off-axis radiation  $RA(\theta, \phi)$  is not a delta.
- For example, if the angular response is a gaussian beam with s.d.  $\sigma$ , the corresponding multipoles transform is
- The detected signal will be:

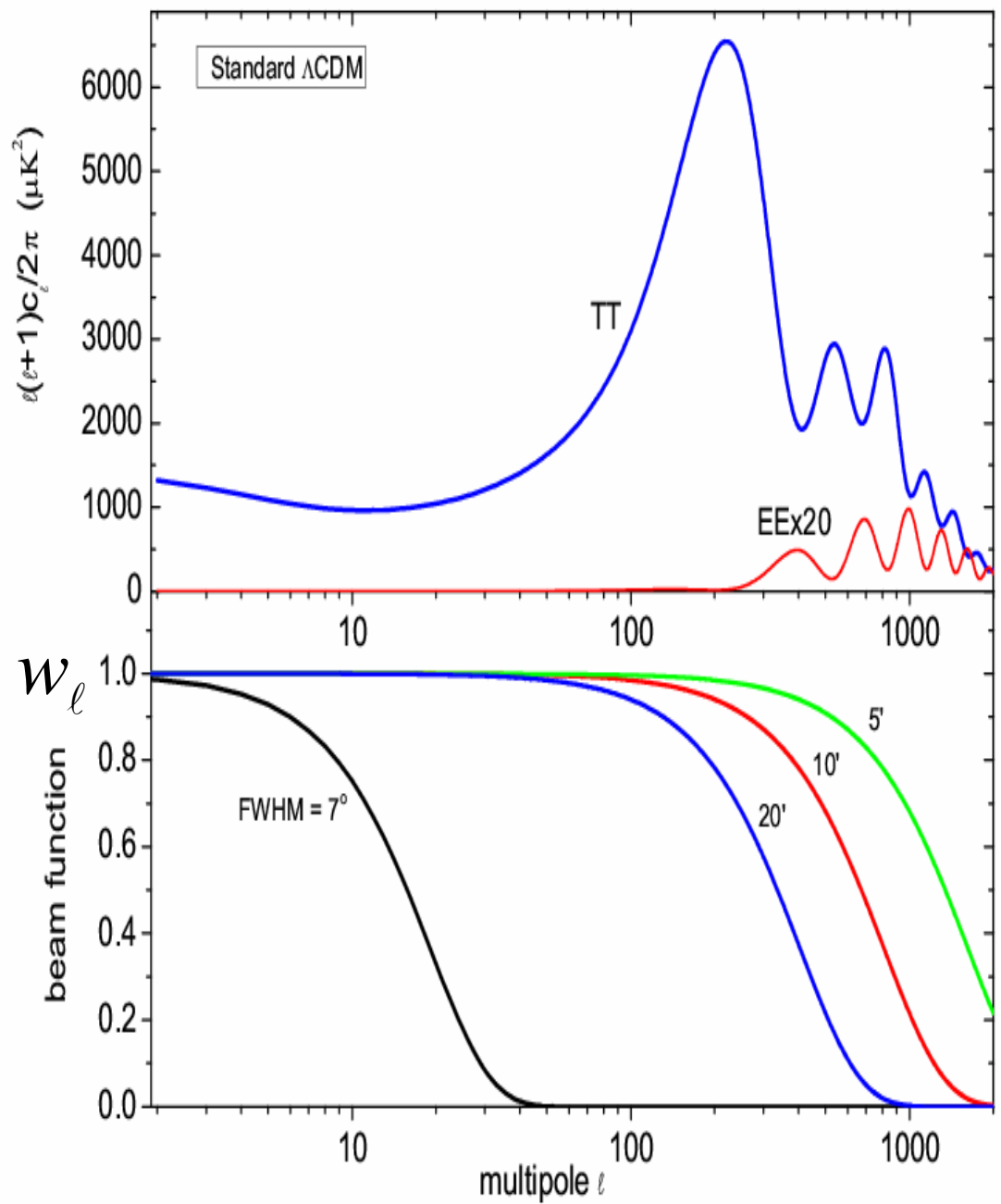
$$w_\ell^{LP} = e^{-\ell(\ell+1)\sigma^2}$$
$$\langle \Delta T^2 \rangle_{meas} = \frac{1}{4\pi} \sum_\ell (2\ell + 1) w_\ell c_\ell$$

$$\frac{\Delta T}{T} = \sum a_{\ell,m} Y_{\ell}^m(\theta, \phi)$$

$$c_{\ell} = \langle a_{\ell,m}^2 \rangle$$

**CAMB code**

<http://camb.info/>

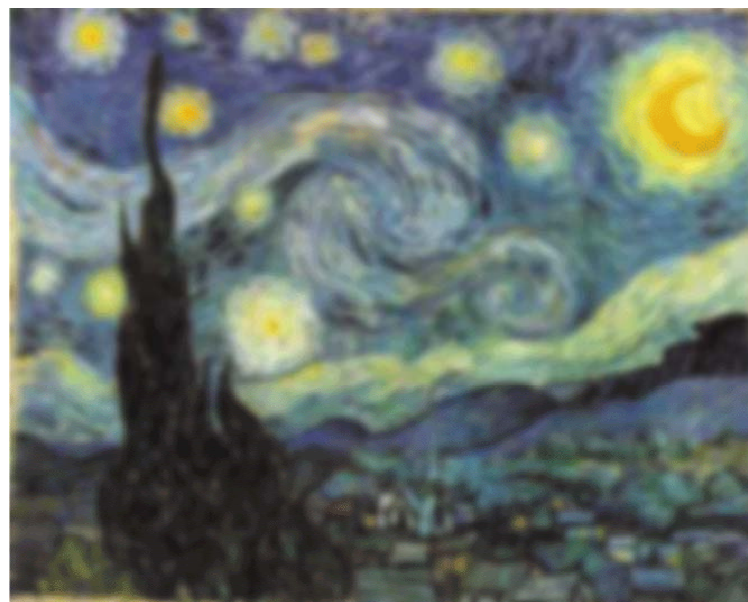


“Starry Night” as Seen by:

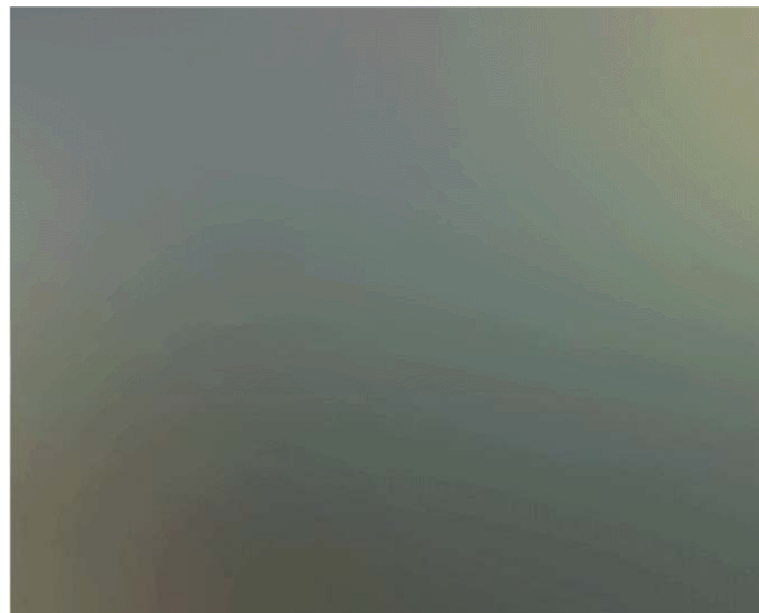
$1^\circ$   
↔



**Van Gogh**



**BOOMERanG** (12' resolution)



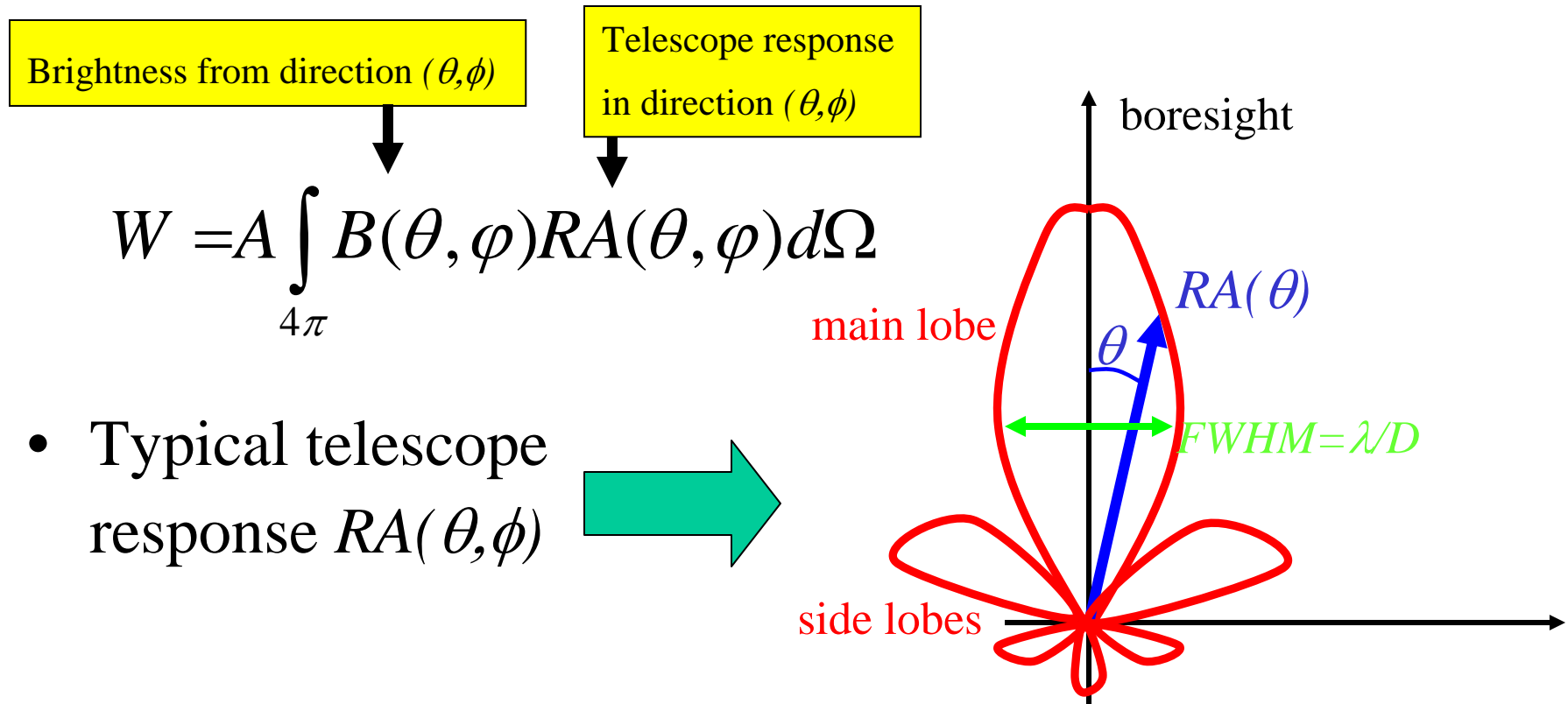
**COBE** (10° resolution)

# Telescopes for the CMB

- Large dimensions of the optical system collecting CMB radiation are required for two reasons :
  - To limit diffraction and detect small structures in the CMB sky
  - To limit far sidelobes and reject strong signals from the ground and other hot sources.

# Importance of low sidelobes

- The power detected is the integral of the brightness times the solid angle, weighted with the angular response of the telescope:



# Importance of low sidelobes

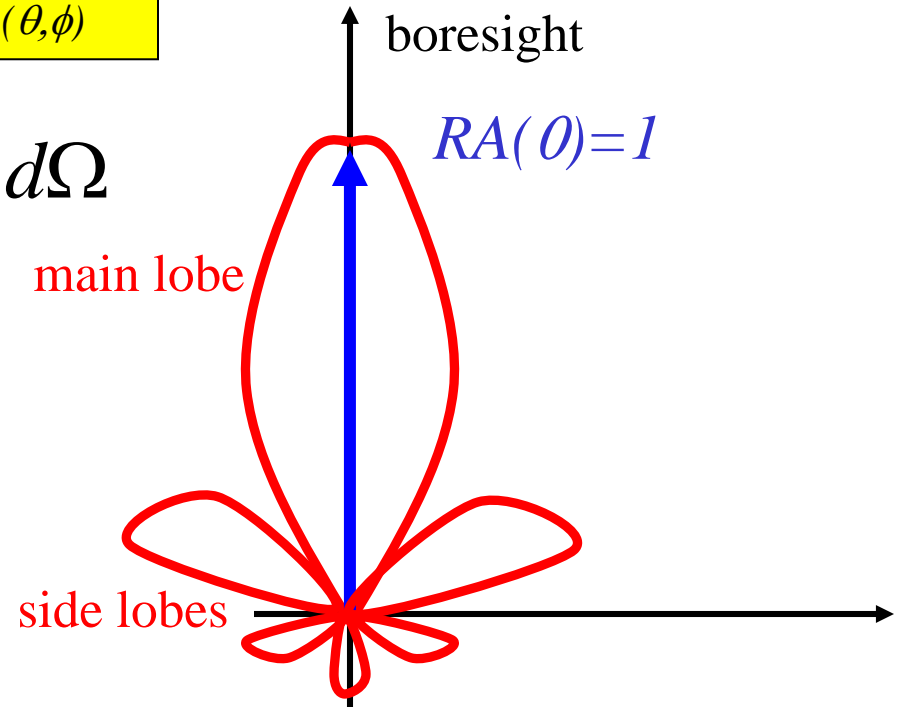
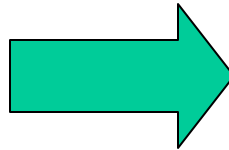
- The power detected is the integral of the brightness times the solid angle, weighted with the angular response of the telescope:

Brightness from direction  $(\theta, \phi)$

Telescope response  
in direction  $(\theta, \phi)$

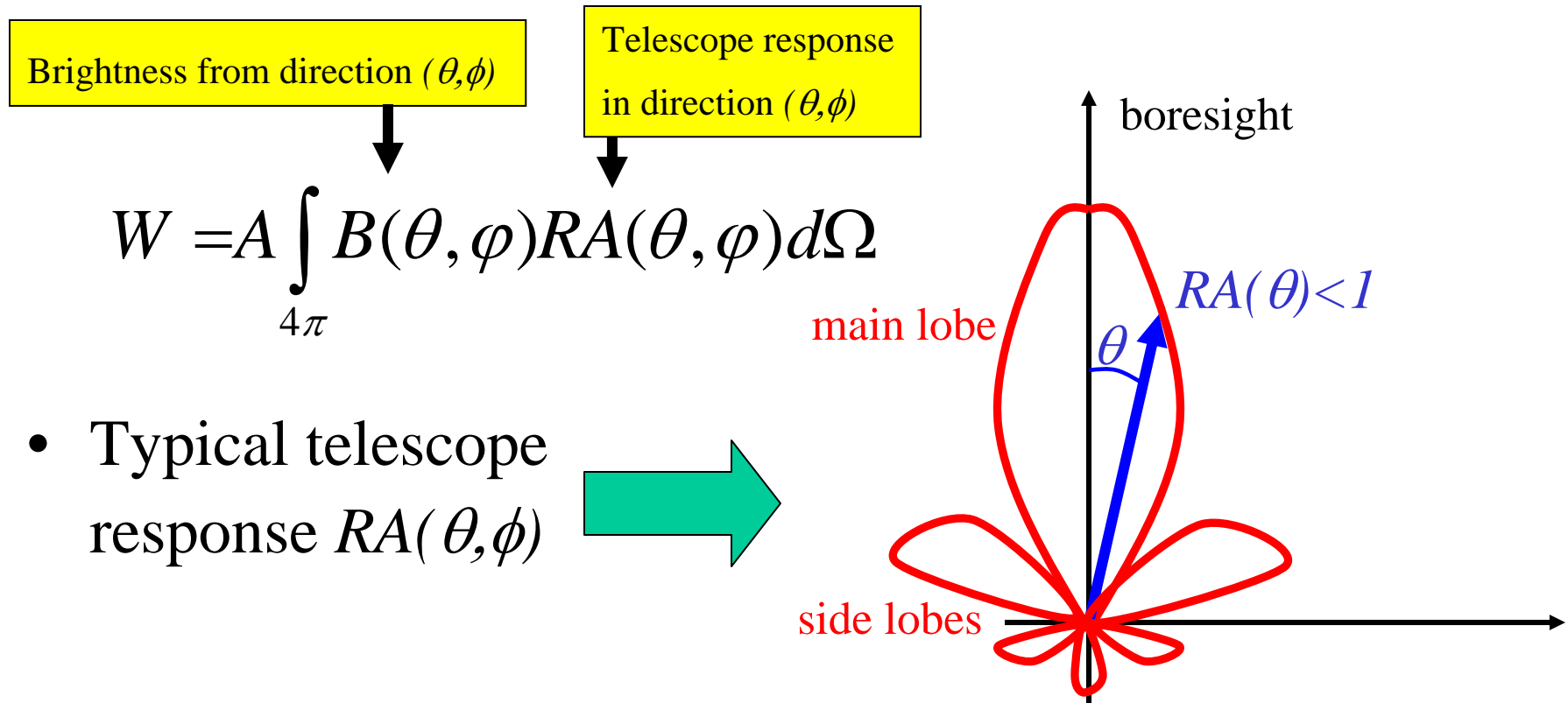
$$W = A \int_{4\pi} B(\theta, \phi) RA(\theta, \phi) d\Omega$$

- Typical telescope response  $RA(\theta, \phi)$



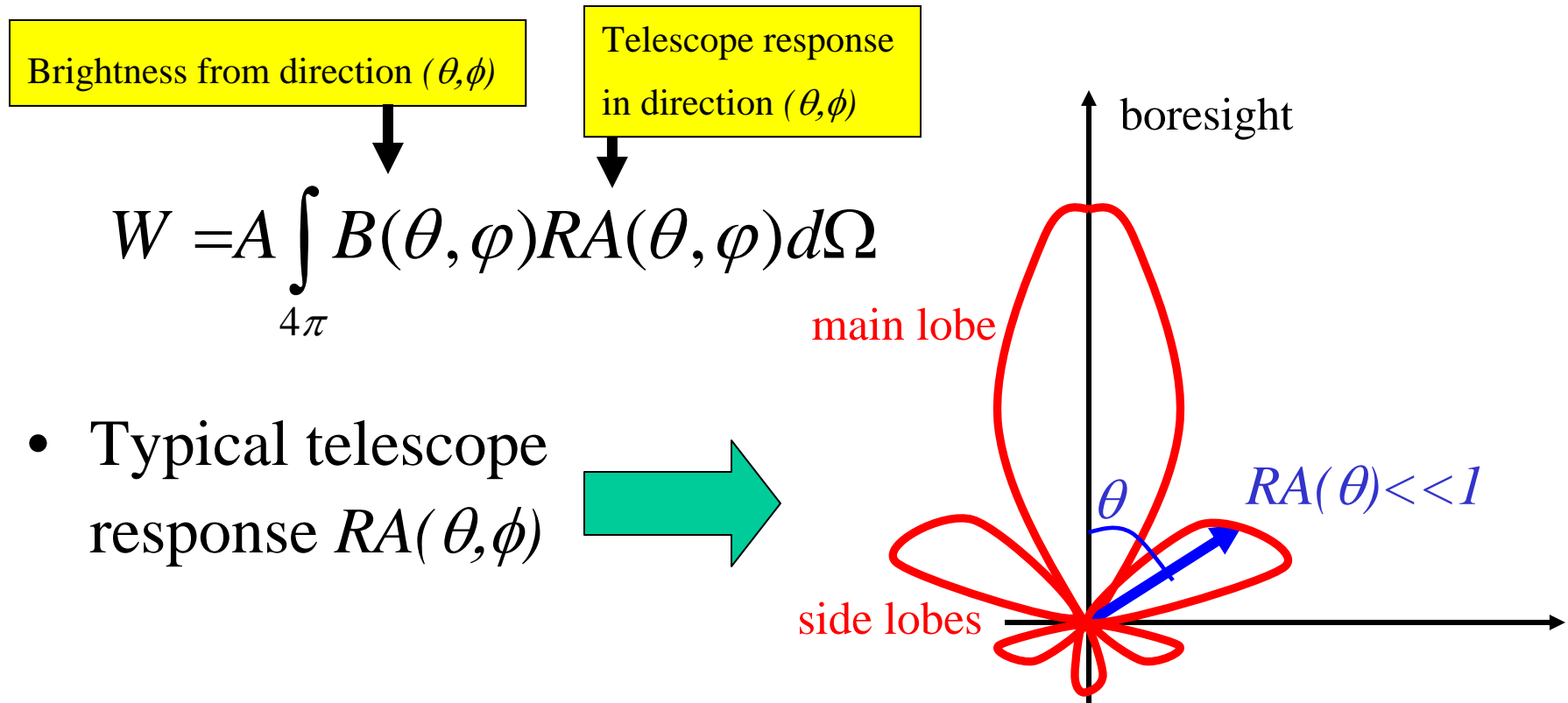
# Importance of low sidelobes

- The power detected is the integral of the brightness times the solid angle, weighted with the angular response of the telescope:



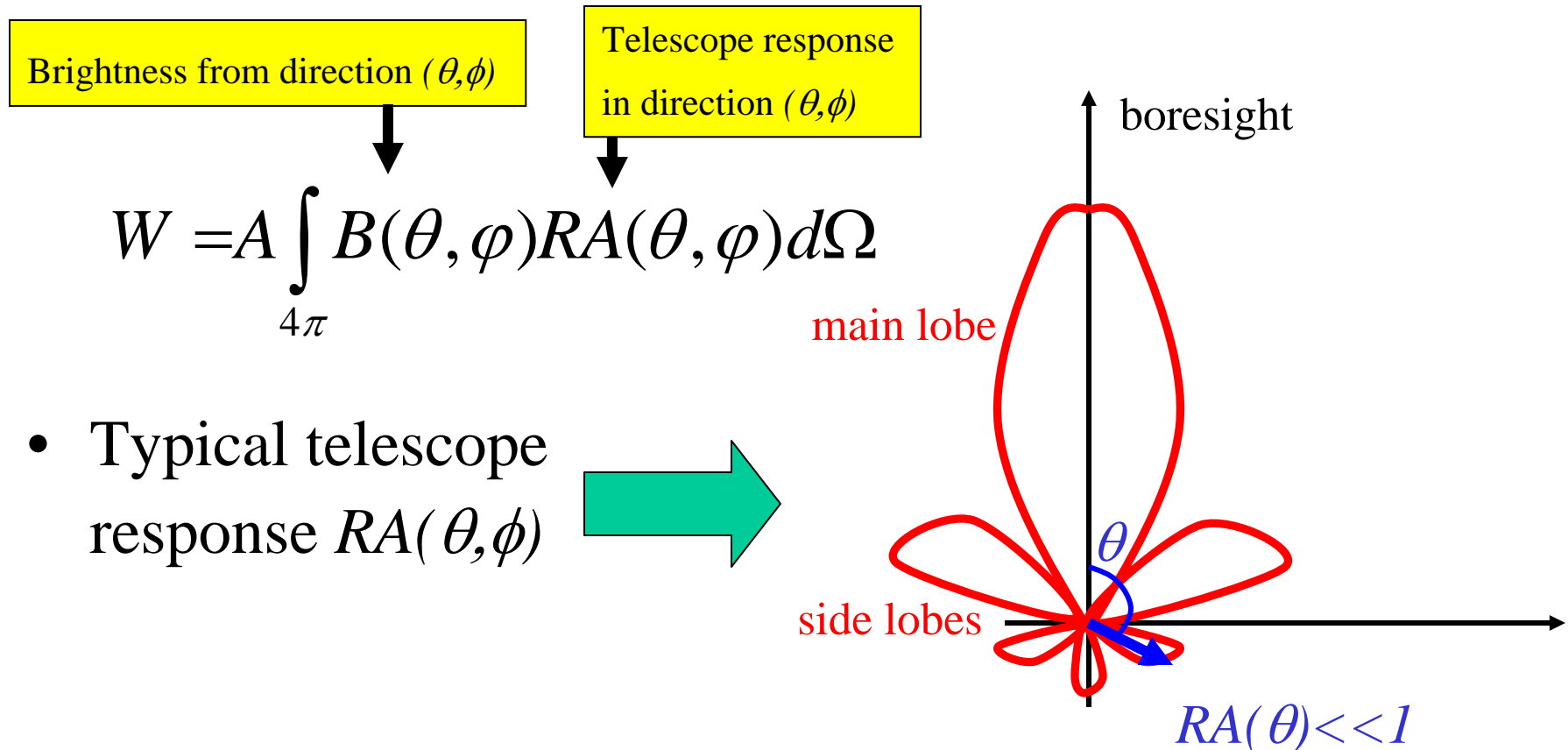
# Importance of low sidelobes

- The power detected is the integral of the brightness times the solid angle, weighted with the angular response of the telescope:



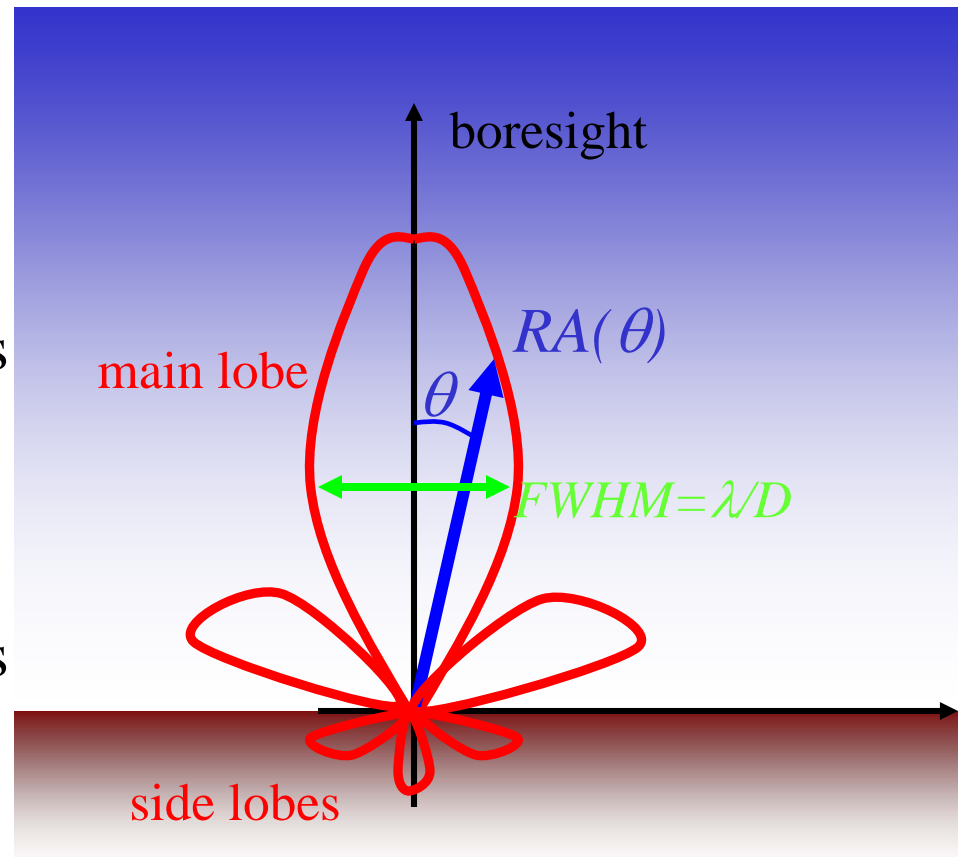
# Importance of low sidelobes

- The power detected is the integral of the brightness times the solid angle, weighted with the angular response of the telescope:



# Importance of low sidelobes

- In the case of CMB observations, the detected brightness is the sum of the brightness from the sky (dominant for the solid angles directed towards the sky, in the main lobe) and the Brightness from the ground (dominant for the solid angles directed towards ground, in the sidelobes).



$$W = A \left[ \int_{\text{main lobe}} B_{\text{sky}}(\theta, \varphi) RA(\theta, \varphi) d\Omega + \int_{\text{side lobes}} B_{\text{Ground}}(\theta, \varphi) RA(\theta, \varphi) d\Omega \right]$$

# Importance of low sidelobes

$$W = A \left[ \int_{\text{main lobe}} B_{\text{sky}}(\theta, \varphi) RA(\theta, \varphi) d\Omega + \int_{\text{side lobes}} B_{\text{Ground}}(\theta, \varphi) RA(\theta, \varphi) d\Omega \right]$$

signal of interest

disturbance signal

$$W \approx A \left[ B_{\text{sky}}(\theta, \varphi) \left\langle RA_{\text{main lobe}}(\theta, \varphi) \right\rangle \Omega_{\text{main lobe}} + B_{\text{Ground}}(\theta, \varphi) \left\langle RA_{\text{side lobes}}(\theta, \varphi) \right\rangle \Omega_{\text{side lobes}} \right]$$

↓

$\approx 3K$

↓

$\approx 1$

↓

$\ll 1 \text{ srad}$

↓

$\approx 300K$

↓

$\approx 2\pi \text{ srad}$

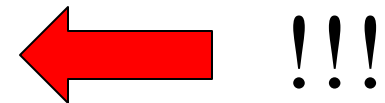
signal of interest  $\gg$  disturbance signal requires

$$\left\langle RA_{\text{main lobe}}(\theta, \varphi) \right\rangle \gg \gg \left\langle RA_{\text{side lobes}}(\theta, \varphi) \right\rangle$$

$$W \approx A \left[ \begin{array}{l} \text{signal of interest} \\ B_{sky}(\theta, \varphi) \langle RA_{main\ lobe}(\theta, \varphi) \rangle \Omega_{main\ lobe} \\ \downarrow \quad \downarrow \quad \downarrow \\ \approx 3K \quad \approx 1 \quad \ll 1\ srad \end{array} + \begin{array}{l} \text{disturbance signal} \\ B_{Ground}(\theta, \varphi) \langle RA_{side\ lobes}(\theta, \varphi) \rangle \Omega_{side\ lobes} \\ \downarrow \quad \downarrow \\ \approx 300K \quad \approx 2\pi\ srad \end{array} \right]$$

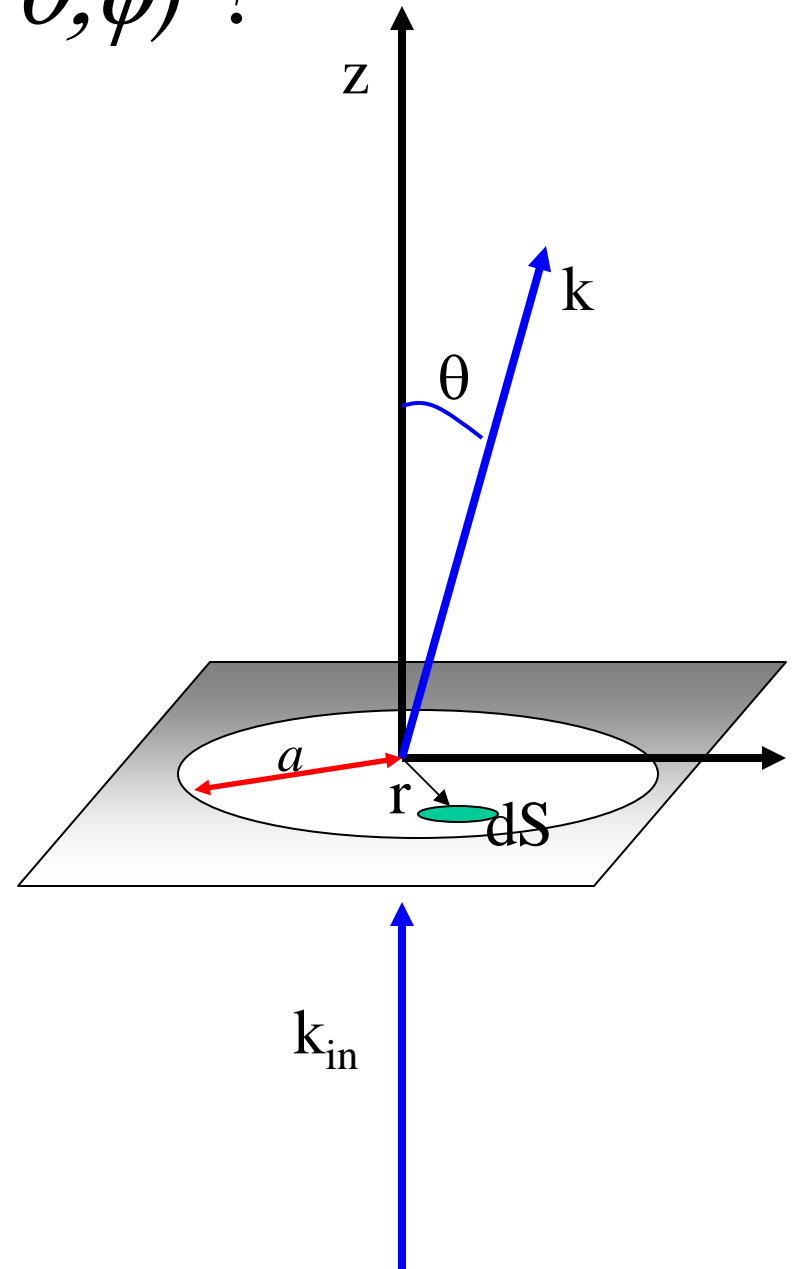
$$\langle RA_{side\ lobes}(\theta, \varphi) \rangle \ll \langle RA_{main\ lobe}(\theta, \varphi) \rangle \left[ \frac{\Omega_{main\ lobe}}{\Omega_{side\ lobes}} \right] \left[ \frac{B_{sky}(\theta, \varphi)}{B_{Ground}(\theta, \varphi)} \right] \approx \frac{\Omega_{main\ lobe} (srad)}{600}$$

FWHM	$\Omega_{mainlobe}$	$\langle RA_{sidelobes} \rangle$
10°	$2 \times 10^{-2}$ srad	$\ll 4 \times 10^{-5}$
1°	$2 \times 10^{-4}$ srad	$\ll 4 \times 10^{-7}$
10'	$7 \times 10^{-6}$ srad	$\ll 1 \times 10^{-8}$
1'	$7 \times 10^{-8}$ srad	$\ll 1 \times 10^{-10}$



# What is $RA(\theta, \phi)$ ?

- Fraunhofer diffraction from a circular aperture (radius  $a$ ) (at large distances from shield)
- The incident wave is an infinite plane wave (wavevector  $\mathbf{k}_{in}$  parallel to the  $z$  axis).
- The outgoing wave is not infinite, and for this very reason it will have components with wavevectors  $\mathbf{k}$  in different directions. So it is not a plane wave.
- We want to find out which are the amplitudes of the different components of the outgoing wave.

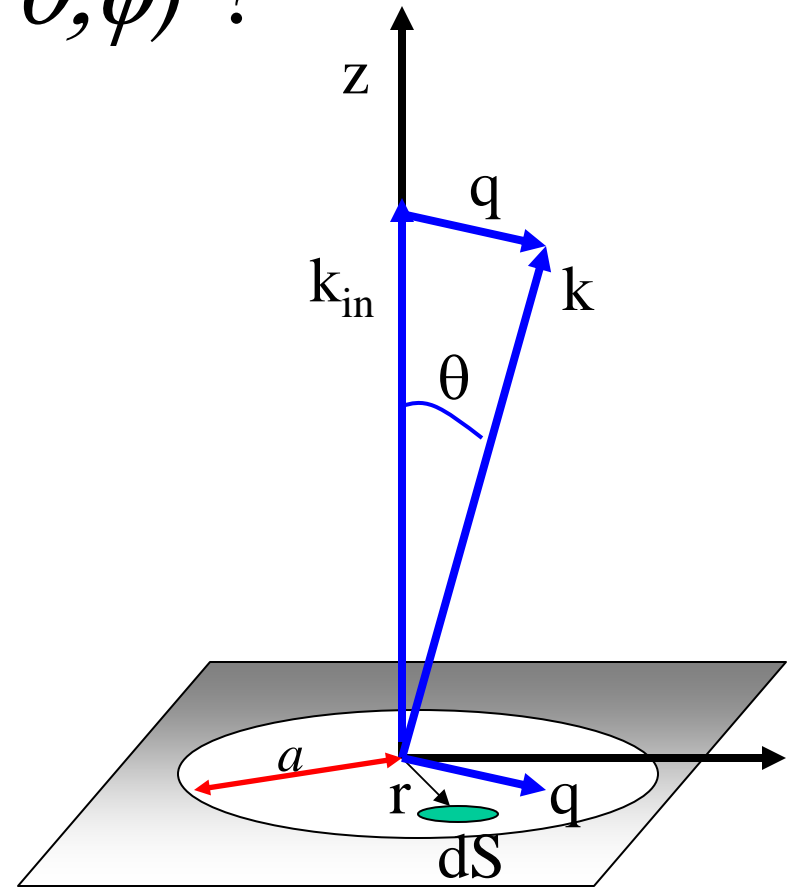


# What is $RA(\theta, \phi)$ ?

- For small angles  $\theta$  the vector  $q = k - k_{in}$  is in the plane of the aperture and  $q = k\theta$ .
- The diffracted component with wavevector  $k$  is the sum of the contributions from all the elements  $dS$  of the aperture, each with its own phase:

$$u_q = \iint_S u_o e^{-i\vec{q} \cdot \vec{r}} dS$$

$$u_q = u_o \int_0^a \int_0^{2\pi} e^{-iqr \cos \varphi} r d\varphi dr = 2\pi u_o \int_0^a J_0(qr) r dr = u_o \frac{2J_1(aq)}{aq}$$



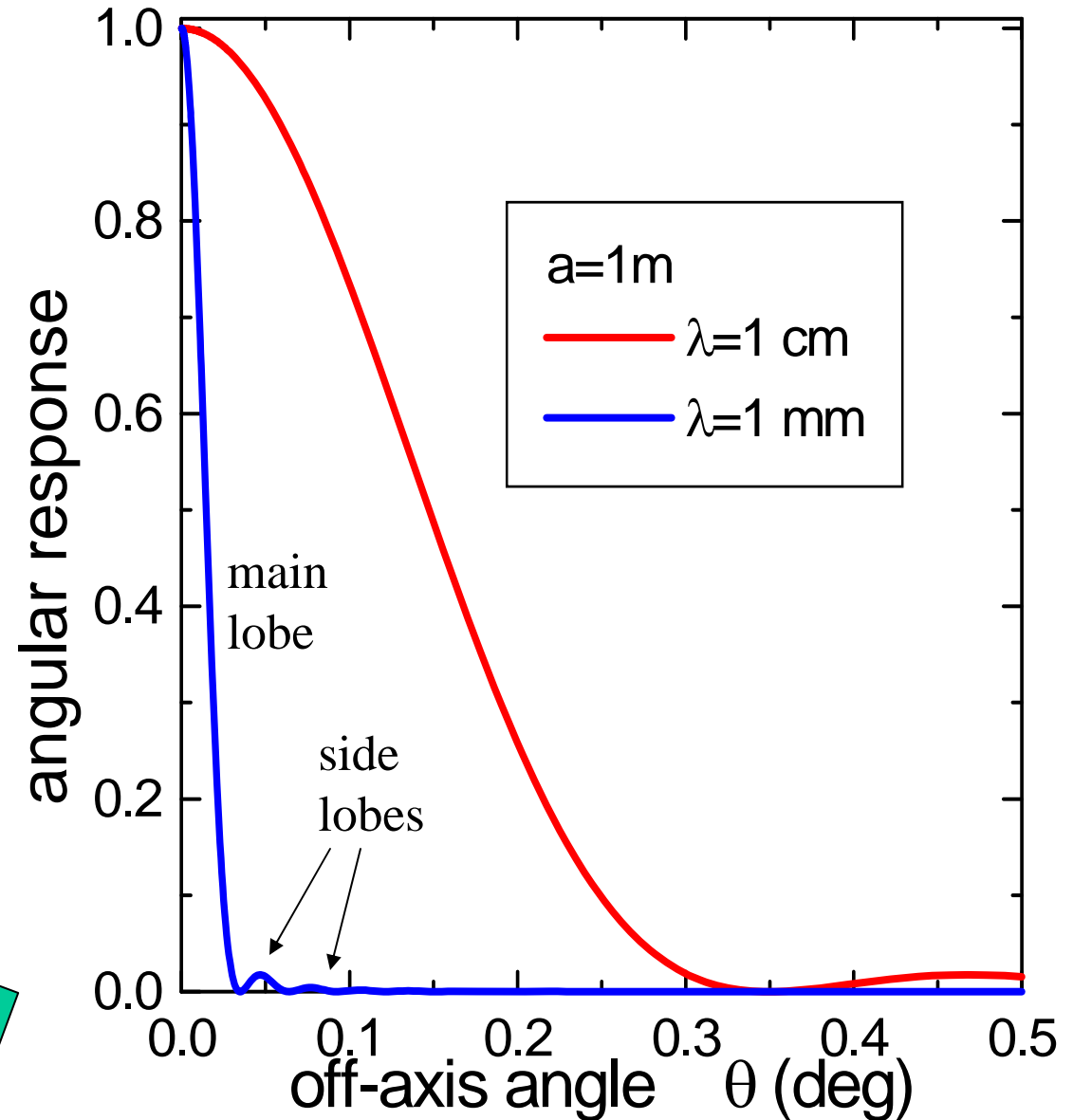
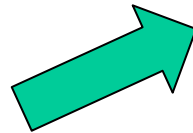
Bessel functions

# What is $RA(\theta, \phi)$ ?

- The intensity is the square of the field:

$$\frac{dI}{d\Omega} = I_o \left[ \frac{2J_1(ak\theta)}{ak\theta} \right]^2$$

- Example: a 2m diameter mirror used at 1 cm and at 1 mm

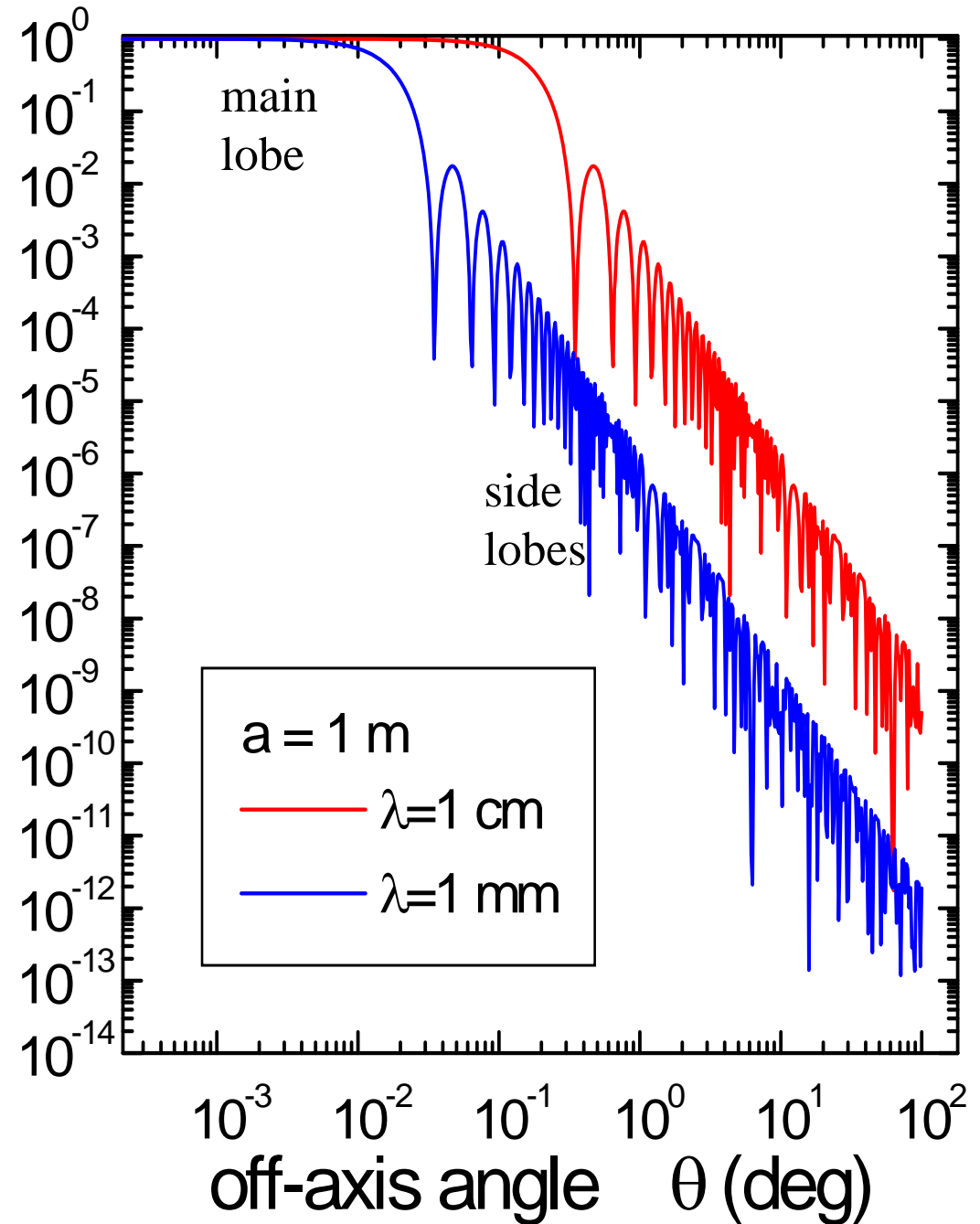


# What is $RA(\theta, \phi)$ ?

- The intensity is the square of the field:

$$\frac{dI}{d\Omega} = I_o \left[ \frac{2J_1(ak\theta)}{ak\theta} \right]^2$$

angular response



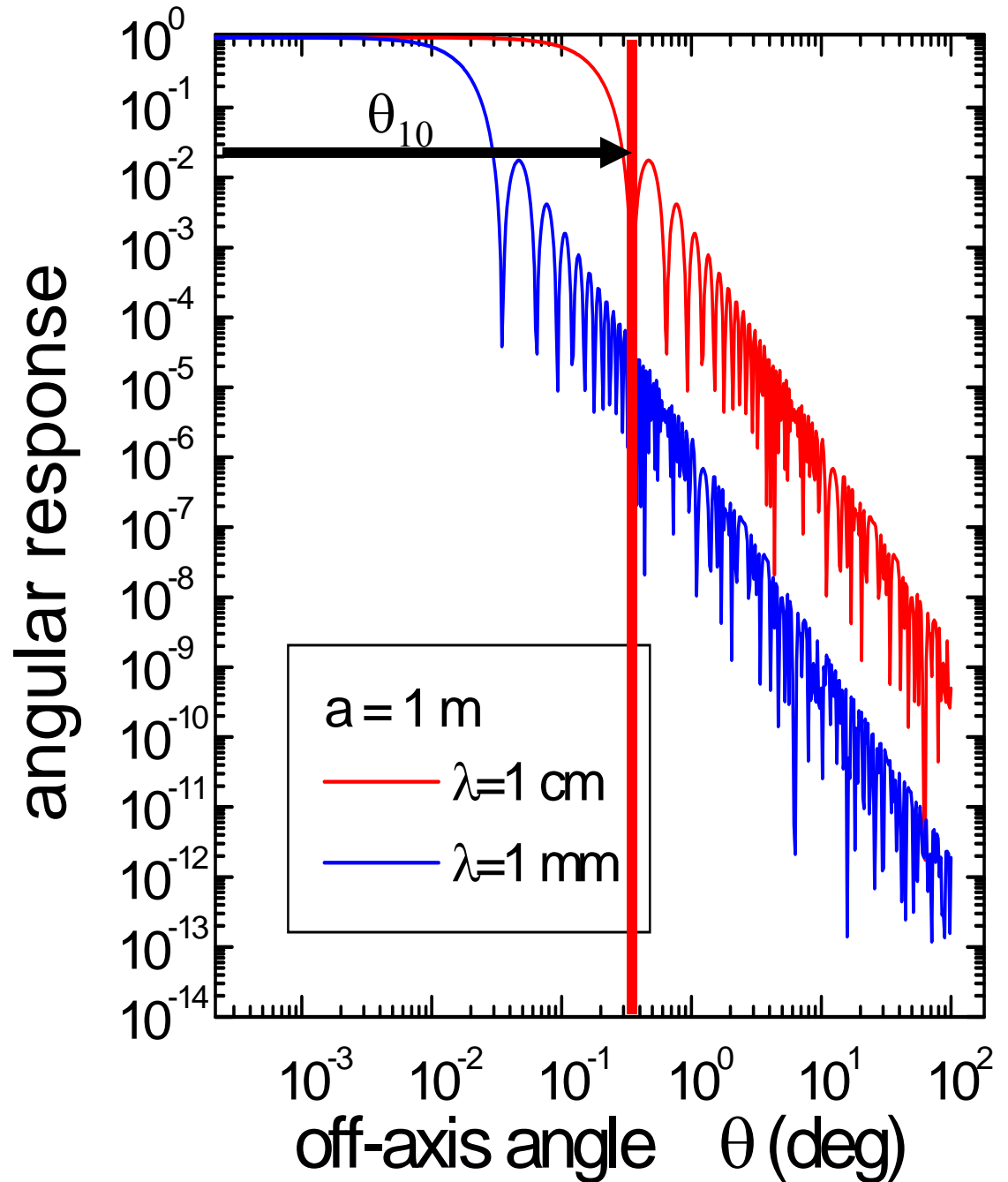
# What is $RA(\theta, \phi)$ ?

- The intensity is the square of the field:

$$\frac{dI}{d\Omega} = I_o \left[ \frac{2J_1(ak\theta)}{ak\theta} \right]^2$$

- The first zero is for

$$\theta_{10} = 1.22 \frac{\lambda}{2a}$$



# What is $RA(\theta, \phi)$ ?

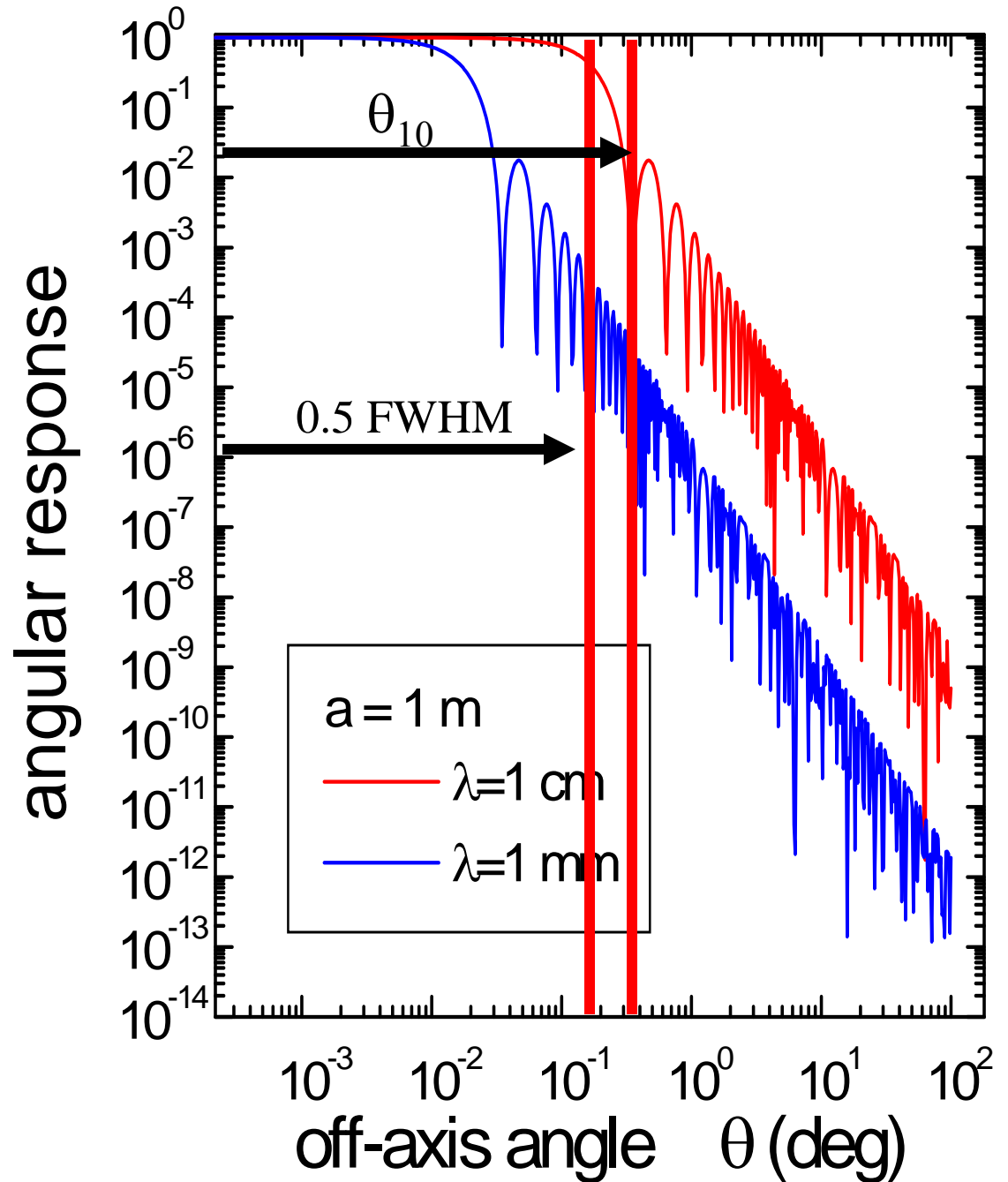
- The intensity is the square of the field:

$$\frac{dI}{d\Omega} = I_o \left[ \frac{2J_1(ak\theta)}{ak\theta} \right]^2$$

- The first zero is for

$$\theta_{10} = 1.22 \frac{\lambda}{2a}$$

- The FWHM is similar

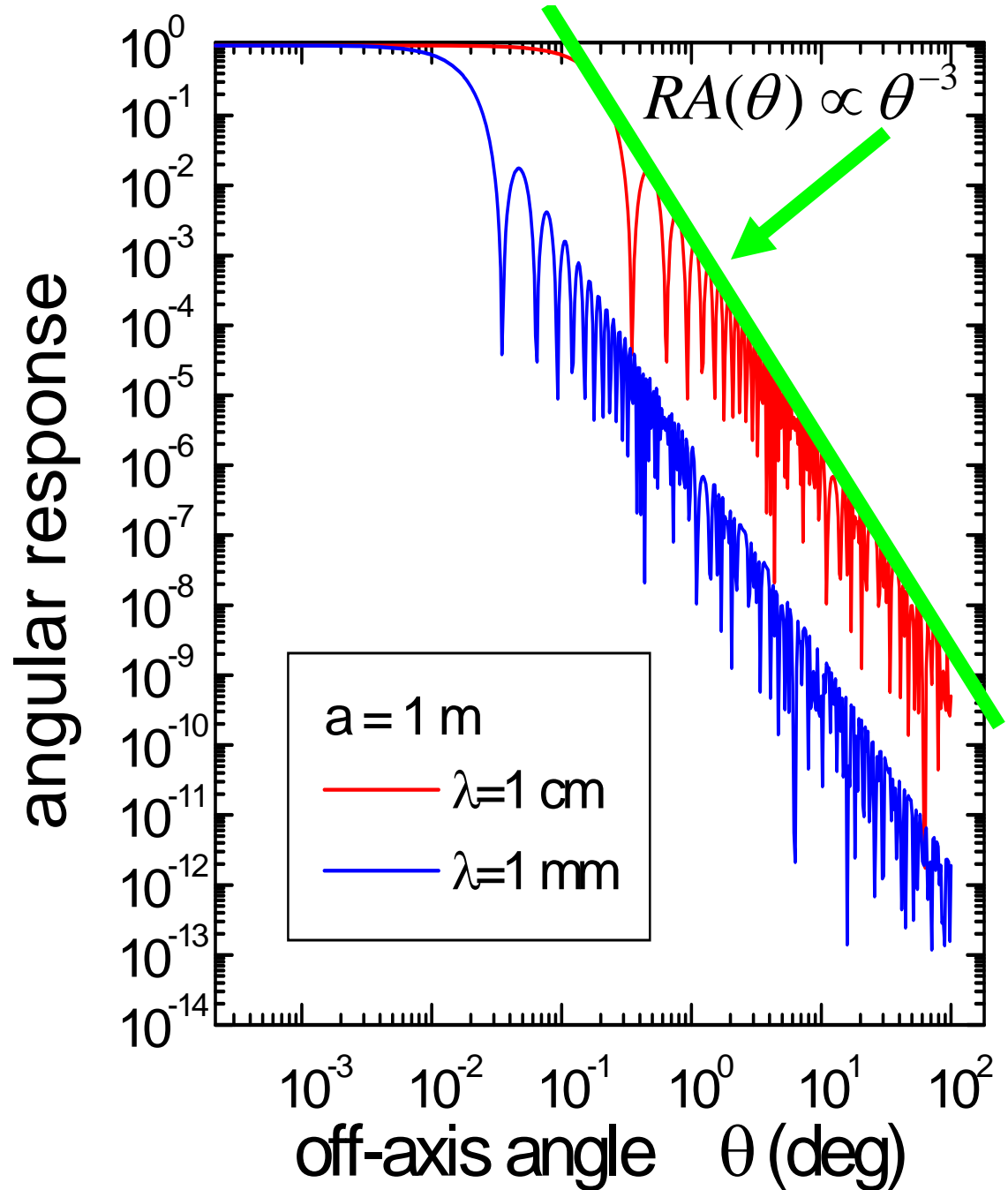


# What is $RA(\theta, \phi)$ ?

- The intensity is the square of the field:

$$\frac{dI}{d\Omega} = I_o \left[ \frac{2J_1(ak\theta)}{ak\theta} \right]^2$$

- The envelope of the off-axis response scales as  $\theta^{-3}$  approximately starting from 0.5 at the FWHM



# exercise

- For the angular response of a circular aperture, compare the power in the main lobe to the power in the sidelobes
- Hint:

$$\frac{P_{side\ lobes}}{P_{main\ lobe}} = \frac{2\pi A \int_{0.61\lambda/a}^{\pi} B_{side\ lobes} \left[ \frac{2J_1(ak\theta)}{ak\theta} \right]^2 \sin\theta d\theta}{2\pi A \int_0^{0.61\lambda/a} B_{main\ lobe} \left[ \frac{2J_1(ak\theta)}{ak\theta} \right]^2 \sin\theta d\theta}$$

- But use approximated formulas ...

# Low diffraction design

- Real world angular responses are worse than the one studied here.
- Sharp edges are in general important sources of diffraction, and must be avoided in low sidelobes design. Use smoothed edges.
- A trumpet has a slow transition to free space at the aperture to avoid diffraction of sound waves.
- The spider supporting the secondary mirror in a Cassegrain telescope is an important source of diffraction.
- Penzias and Wilson used an under-illuminated off-axis paraboloid, to get low sidelobes

10dB = a factor 10 in power

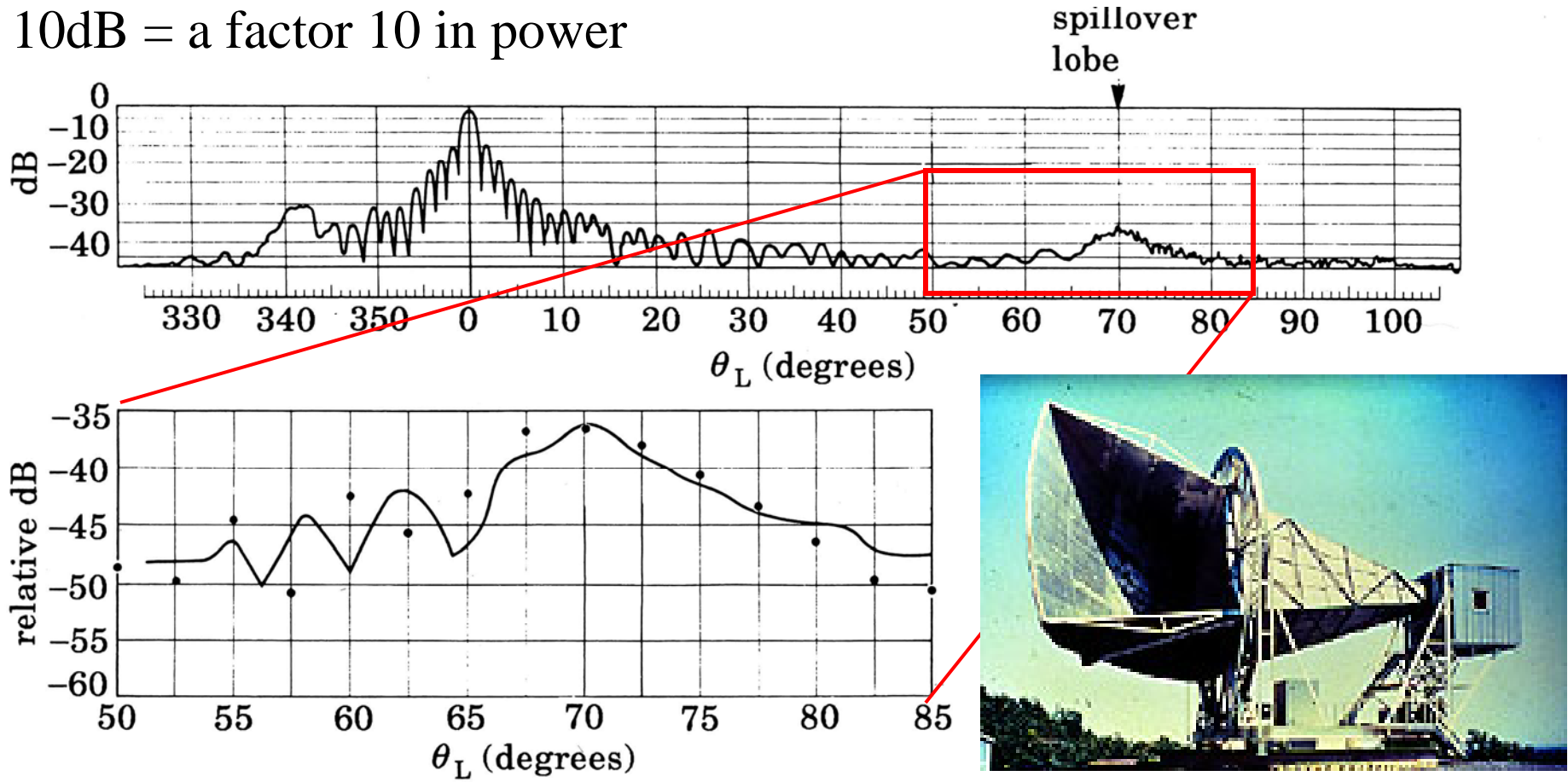
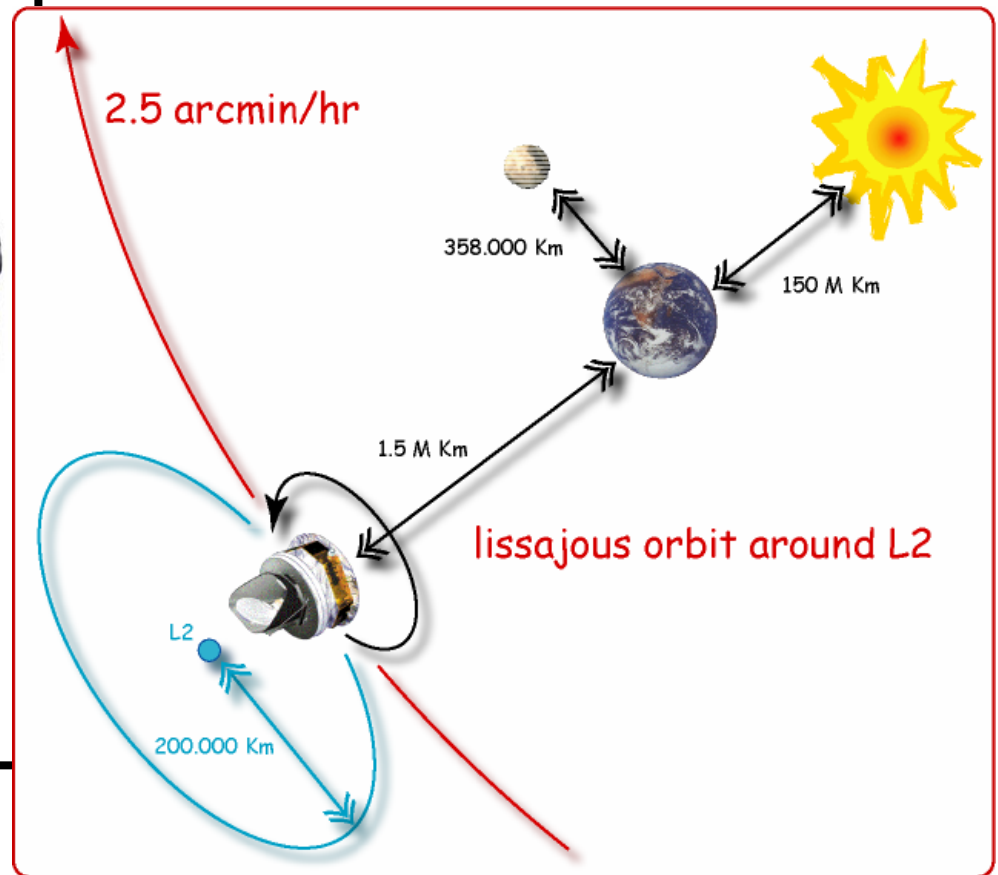
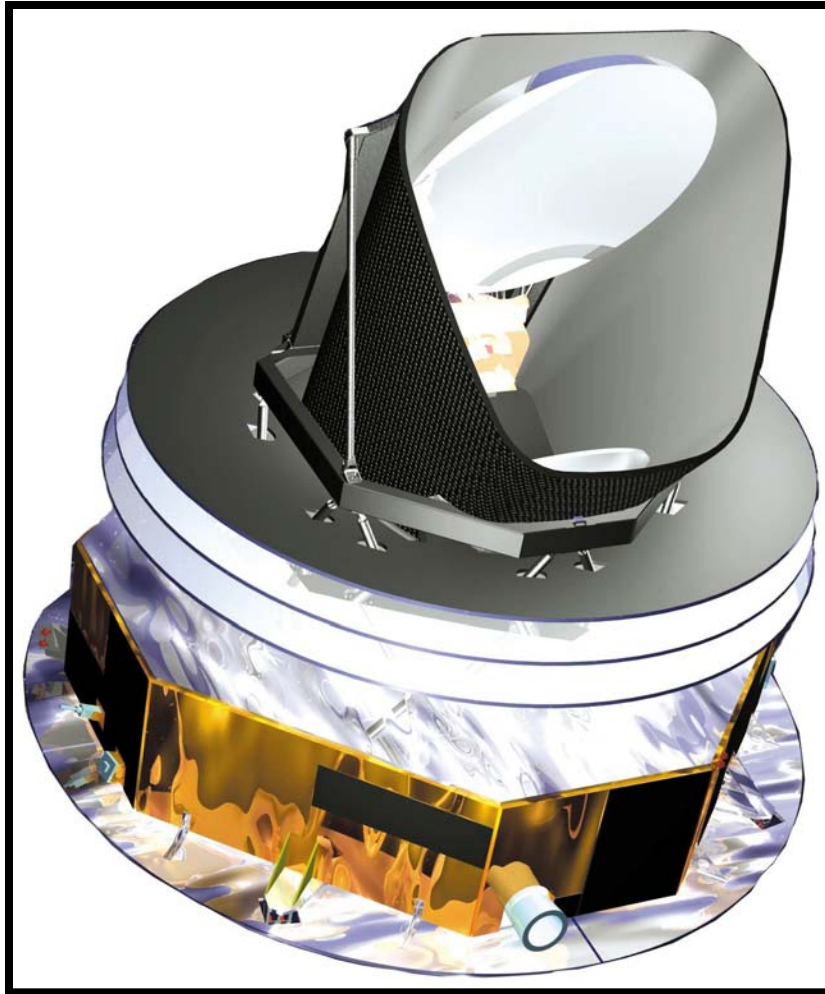
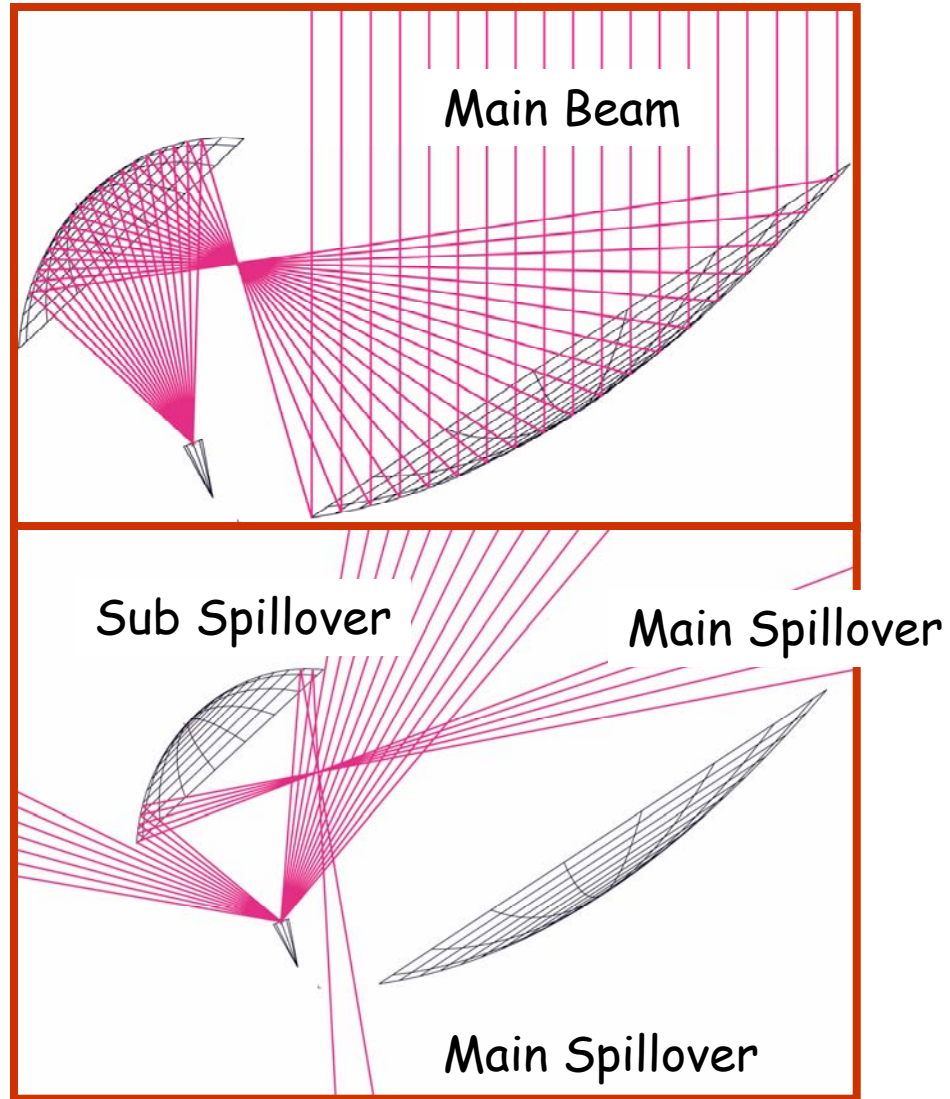


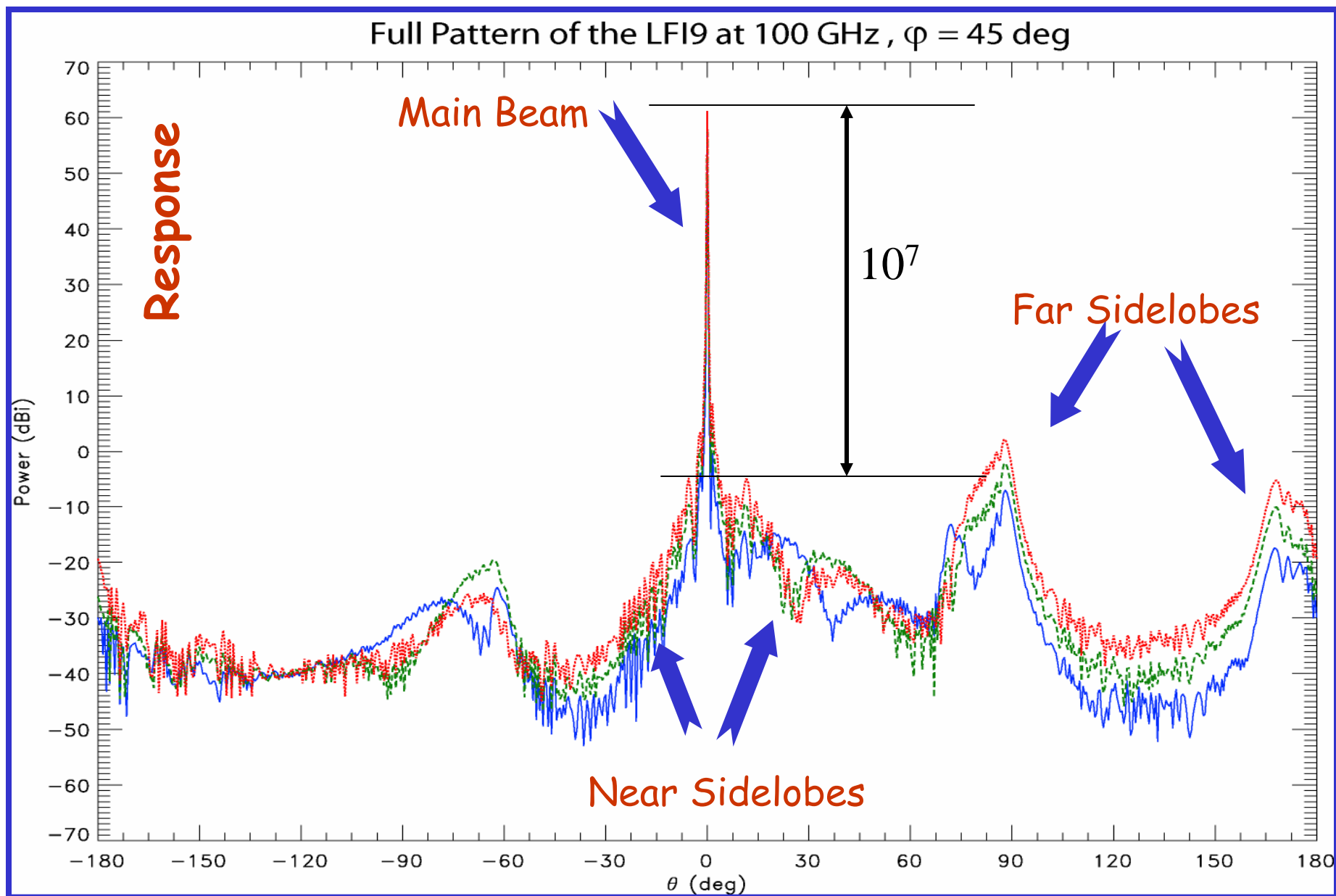
Fig. 12. – Upper panel: scheme of the horn-antenna. It is a part of a large paraboloid: lateral shields prevent spurious radiation entering in the system outside the nominal beam width. Isotropic level  $-43$  dB. Lower panel: angular response of the antenna, as measured by means of a transmitter located in front of the antenna at different angles. The spillover lobe is studied in detail in the lowest part of the graph. Earth's radiation entering via the spillover lobe determines the antenna temperature noise. — Measured data, ● computed data. (Adapted by Crawford *et al.* [34].)

# Other example of low sidelobes design: Planck



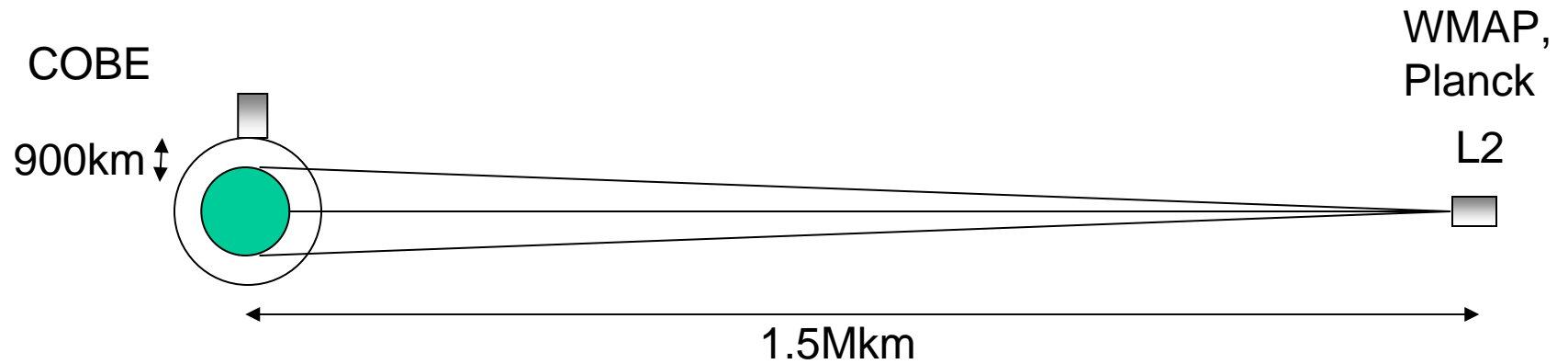
# STRAY LIGHT





Angle from boresight

F. Villa, LFI



Going to L2 reduces the solid angle occupied by the Earth by a factor  $2\pi/2 \times 10^{-4} = 31000$ , thus relaxing by the same factor the required off-axis rejection.

FWHM	$\Omega_{\text{mainlobe}}$	$\langle RA_{\text{sidelobes}} \rangle$
10°	$2 \times 10^{-2}$ sr	$\ll 1$
1°	$2 \times 10^{-4}$ sr	$\ll 0.01$
10'	$7 \times 10^{-6}$ sr	$\ll 3 \times 10^{-4}$
1'	$7 \times 10^{-8}$ sr	$\ll 3 \times 10^{-6}$

# Telescopes for the CMB

- After the COBE-DMR results there was a clear the need for meter-sized telescopes for the CMB.
- Working at high frequencies requires smaller mirrors for the same resolution.
- A 1 m mirror at 150 GHz provides 10' resolution, at 15 GHz provides only  $1.4^\circ$ .
- However atmospheric noise at high frequencies is severe.
- So, waiting for a new space mission, two classes of experiments were developed:
  - Ground-based radiometers working at high altitude mountain sites, at  $\lambda$  around 1 cm
  - Balloon-borne bolometric receivers working at  $\lambda$  around 1-2 mm

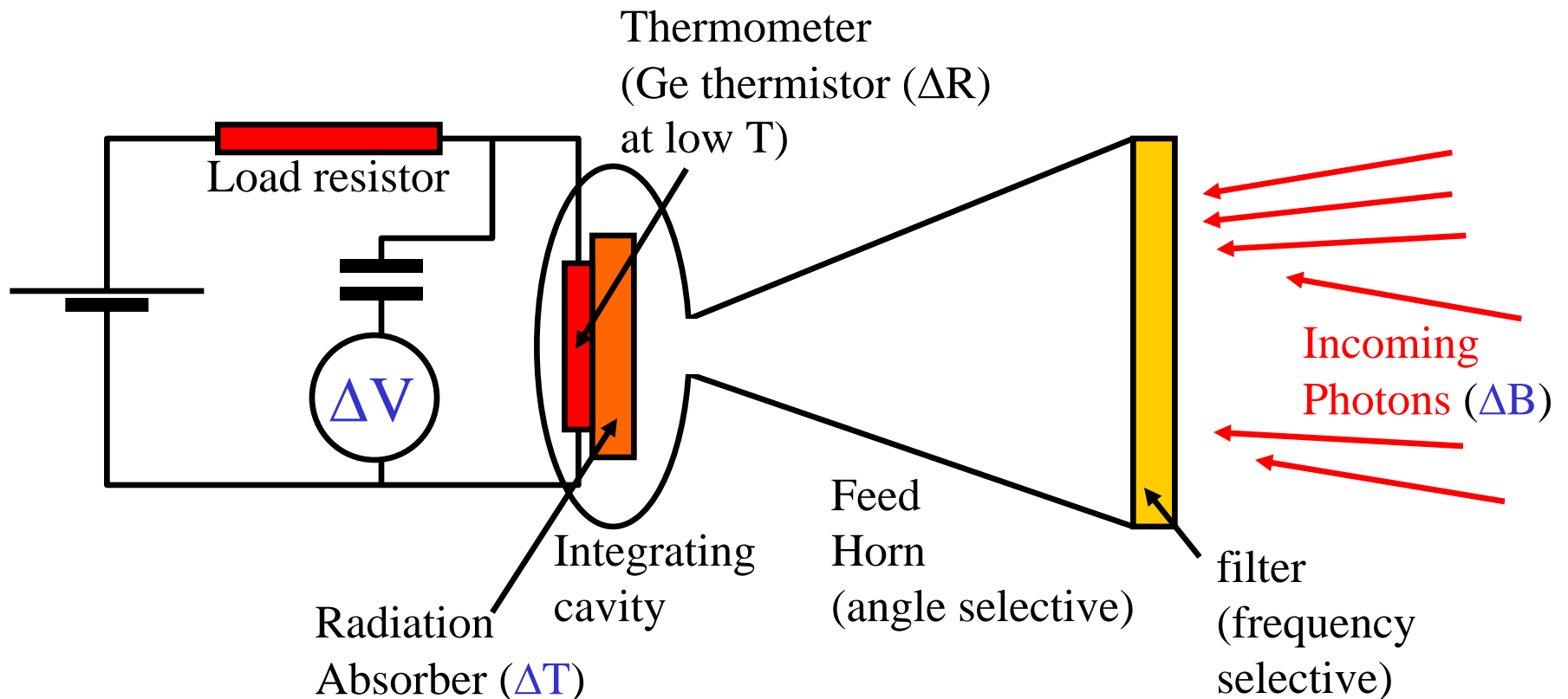
# Detectors

# Detectors

- Coherent detectors measure amplitude and phase of the em wave
- Thermal detectors measure the energy of the em wave
- On both sides, astrophysical and CMB research drove the development of new devices:
  - Cryogenic, ultra-low noise HEMT amplifiers (coherent)
  - Cryogenic “Spider Web” and “Polarization Sensitive” Bolometers (thermal)
  - Low sidelobe corrugated antennas .....
- Also, the two worlds are progressively mixed: for example waveguides and striplines are now used with cryogenic bolometers

# Cryogenic Bolometers

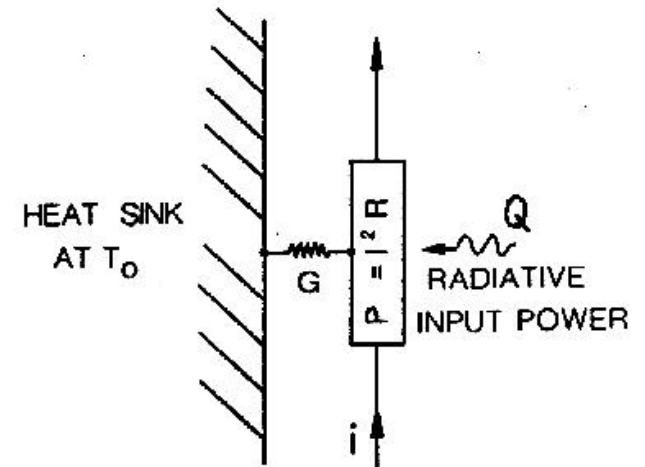
- The CMB spectrum is continuum and bolometers are wide band detectors. That's why they are so sensitive.



- Fundamental noise sources are Johnson noise in the thermistor ( $\langle \Delta V^2 \rangle = 4kTR\Delta f$ ), temperature fluctuations in the thermistor ( $\langle \Delta W^2 \rangle = 4kGT^2\Delta f$ ), background radiation noise ( $T_{\text{bkg}}^5$ ) → need to reduce the temperature of the detector and the radiative background.

# Cryogenic Bolometers

- In steady conditions the temperature rise of the sensor is due to the background radiative power absorbed  $Q$  and to the electrical bias power  $P$ :

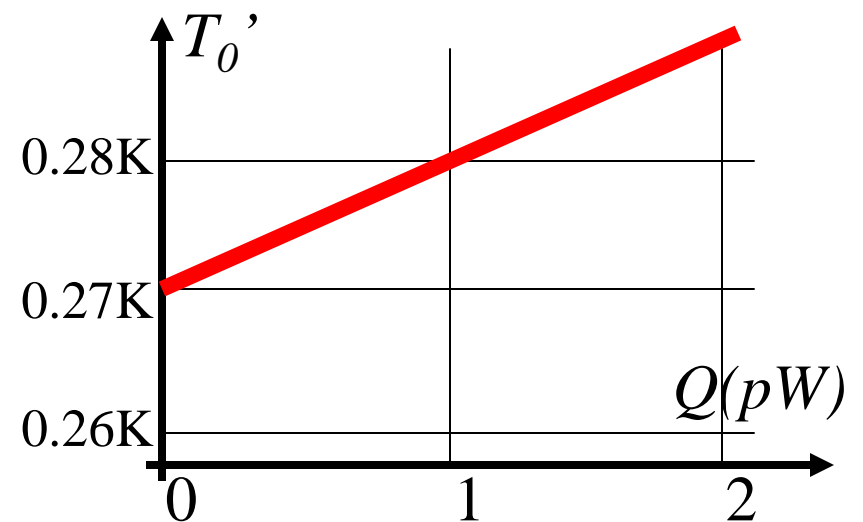


$$G(T - T_0) = Q + P$$

- The effect of the background power is thus equivalent to an increase of the reference temperature:

$$P = G \left[ T - \left( T_0 + \frac{Q}{G} \right) \right] = G(T - T_0')$$

$$T_0' = T_0 + \frac{Q}{G}$$



# Cryogenic Bolometers

- In presence of an additional signal  $\Delta Q e^{j\omega t}$  (from the sky)

$$C \frac{d\Delta T}{dt} + G_{eff} \Delta T = \Delta Q \quad \rightarrow$$

$$\left| \frac{dT}{dQ} \right| = \frac{1}{G_{eff} \sqrt{1 + \tau^2 \omega^2}}$$

$$\tau = \frac{C}{G}$$

- There is a tradeoff between high sensitivity and fast response. **The heat capacity  $C$  should be minimized** to optimize both  $\rightarrow$
- Using a current biased thermistor to readout the temperature change:

Small sensor at **low temperature**

$$\alpha = \frac{1}{R(T)} \frac{dR(T)}{dT} \Rightarrow dV = i dR = i \alpha R dT$$

Responsivity  $\rightarrow$

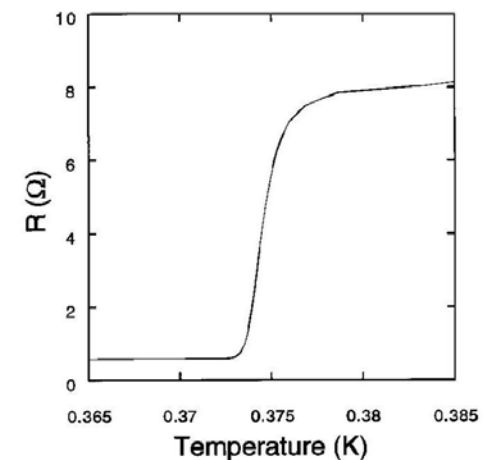
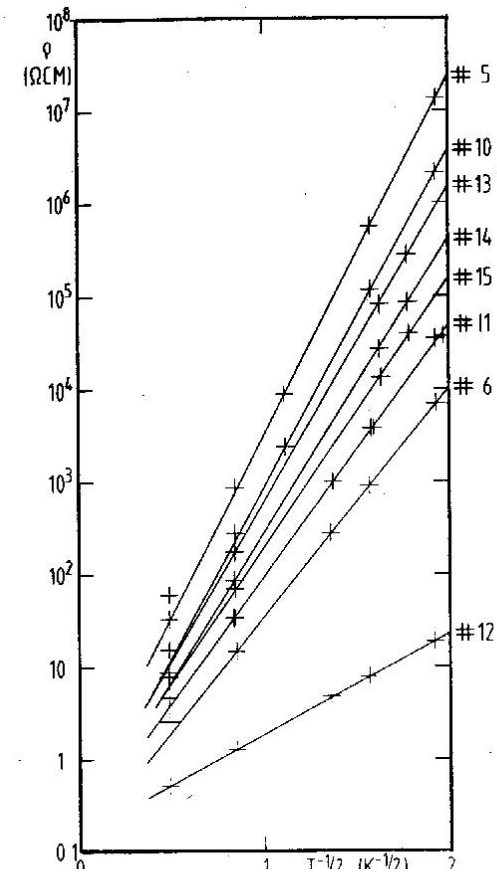
$$\mathfrak{R} = \frac{dV}{dQ} = i \alpha R \frac{dT}{dQ} = \frac{i \alpha R}{G_{eff} \sqrt{1 + \tau^2 \omega^2}}$$

# Cryogenic Bolometers

$$\alpha = \frac{1}{R(T)} \frac{dR(T)}{dT}$$

$$\Re = \frac{i\alpha R}{G_{eff} \sqrt{1 + \tau^2 \omega^2}}$$

- A large  $\alpha$  is important for high responsivity.
- Ge thermistors:  $\alpha \approx -10 K^{-1}$
- Superconducting transition edge thermistors:  $\alpha \approx 1000 K^{-1}$



# Cryogenic Bolometers

- Johnson noise in the thermistor

$$\frac{d\langle \Delta V_J^2 \rangle}{df} = 4kTR$$

- Temperature noise

$$\frac{d\langle \Delta W_T^2 \rangle}{df} = \frac{4kT^2 G_{eff}}{G_{eff}^2 + (2\pi fC)^2}$$

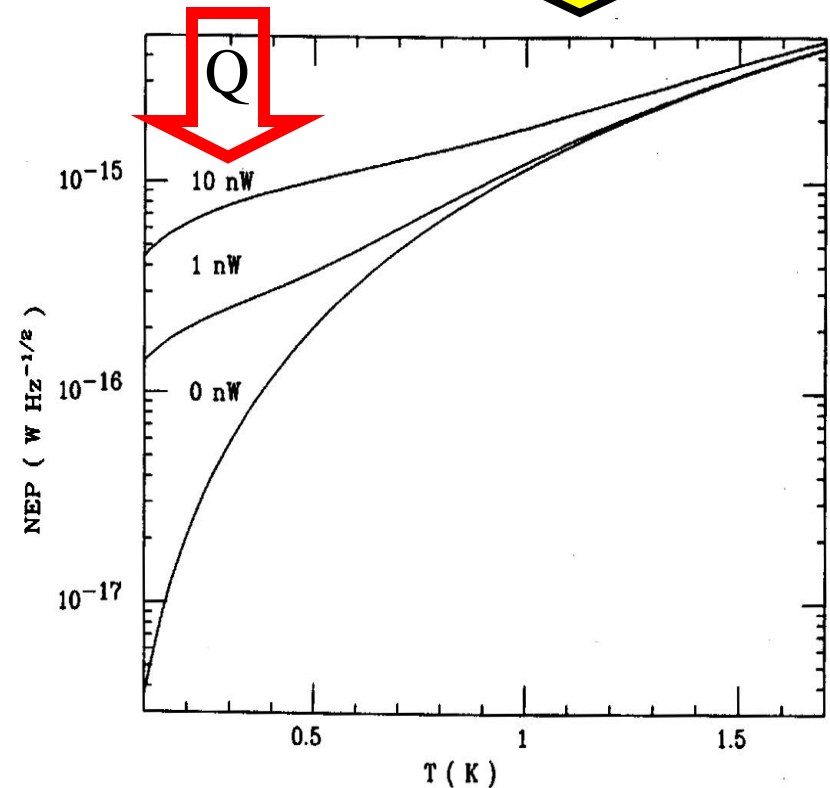
- Photon noise

$$\frac{d\langle \Delta W_{Ph}^2 \rangle}{df} = \frac{4k^5 T_{BG}^5}{c^2 h^3} \int \epsilon \frac{x^4 (e^x - 1 + \epsilon)}{(e^x - 1)^2} dx$$

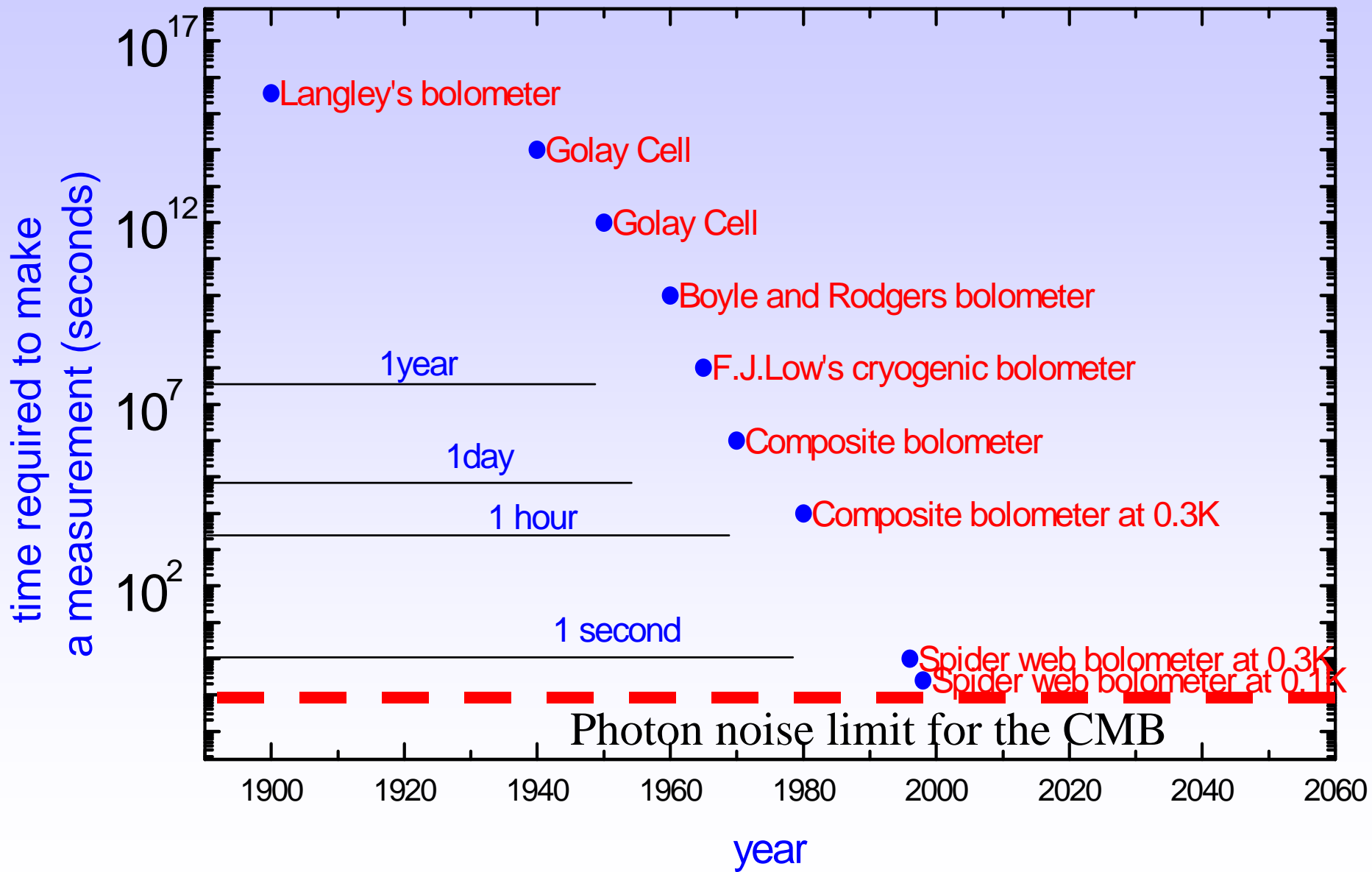
- Total NEP (fundamental): 

$$NEP^2 = \frac{1}{\mathcal{R}^2} \frac{d\langle \Delta V_J^2 \rangle}{df} + \frac{d\langle \Delta W_T^2 \rangle}{df} + \frac{d\langle \Delta W_{Ph}^2 \rangle}{df}$$

Again, need of low temperature and low background



# Development of thermal detectors for far IR and mm-waves



# Spider-Web Bolometers

- The absorber is micro machined as a web of metallized  $\text{Si}_3\text{N}_4$  wires, 2  $\mu\text{m}$  thick, with 0.1 mm pitch.
- This is a good absorber for mm-wave photons and features a very low cross section for cosmic rays. Also, the heat capacity is reduced by a large factor with respect to the solid absorber.
- NEP  $\sim 2 \cdot 10^{-17} \text{ W/Hz}^{0.5}$  is achieved @0.3K
- $150 \mu\text{K}_{\text{CMB}}$  in 1 s
- Mauskopf *et al.* Appl.Opt. **36**, 765-771, (1997)

